LAWRENCE
LIVERMORE
NATIONAL
LABORATORY

LLNL-JRNL-648035

Radioxenon Production and Transport from an Underground Nuclear Detonation to Ground Surface

Y. Sun, C. R. Carrigan, Y. Hao

December 19, 2013

Pure and applied geophysics

Disclaimer

Radioxenon Production and Transport from an Underground Nuclear Detonation to Ground Surface

Yunwei Sun[1], Charles R. Carrigan, Yue Hao
Lawrence Livermore National Laboratory

Abstract

Radioxenon isotopes are considered as possible indicators for detecting and discriminating underground nuclear explosions. To monitor and sample the release of radioxenon isotopes, both independent and chain-reaction yields need to be considered together with multiphase transport in geological systems from the detonation point to the ground surface. For the sake of simplicity, modeling of radioxenon isotopic radioactivities has typically been focused either on chain reactions in a batch reactor without considering multiphase transport or on radionuclide transport with simplified reactions. Although numerical methods are available for integrating coupled differential equations of complex decay networks, the stiffness (with greatly differing decay rates) of ordinary differential equations may require substantial additional effort to obtain solutions for the fully coupled system. For this reason, closed-form solutions for sequential reactions and numerical solutions for multi-parent converging and multi-daughter branching reactions were previously developed and used to simulate xenon isotopic radioactivities in the batch reactor mode. In this paper, we develop a fully-coupled numerical model which involves tracking 24 components (i.e., 22 radionuclide components plus air and water) in two phases to enhance model predictability of simultaneously simulating xenon isotopic transport and fully-coupled chain reactions. To validate the numerical model and verify the corresponding computer code, we derived closed-form solutions for first-order xenon reactions in a batch reactor mode and for single-gas phase transport coupled with the xenon reactions in a one-dimensional column. Finally, cylindrical 3-D simulations of two-phase flow within a dual permeability fracture-matrix medium, simulating the geo-hydrologic regime of an underground nuclear explosion, indicate the existence of both a strong temporal and spatial dependence of xenon isotopic ratios sampled at the surface. In the example presented here, temporally evolving subsurface xenon isotopic ratios are found to migrate cross the discrimination line delineating civilian nuclear activities from an underground nuclear explosion in the Kalinowski Multi-Isotope Ratio Chart.

Keywords: Reactive transport, Decay, Ingrowth, First-order reaction, Isotopic ratio.

[1]Corresponding author, Lawrence Livermore National Laboratory
Livermore, CA 94550, U.S.A. E-mail address: sun4@llnl.gov

1. Introduction

Radioxenon isotopes, ^{131m}Xe, ^{133m}Xe, ^{133}Xe, and ^{135}Xe, are considered as candidate indicators for detecting underground nuclear explosions (Bowyer et al., 2002; Kalinowski et al., 2010; Kalinowski, 2011; Lowrey et al., 2012, 2013). To discriminate an explosion-induced signature from that of civilian sources, it is necessary to study the xenon production mechanism from a nuclear explosion and the transport to the ground surface. Due to the complexity of radioactive decay-chain networks, the xenon-source term from a nuclear explosion was previously estimated in multiphase transport models based on detonation yield without considering chain-reaction production (Carrigan et al., 1996; Sun and Carrigan, 2012). On the other hand, chain yields have been modeled in batch reactor mode without considering transport (Kalinowski et al., 2010; Kalinowski, 2011).

Since Bateman (1910), radioactive decay and ingrowth have been often treated as first-order sequential reactions without considering branching and converging connections (e.g., Pigford et al., 1980; van Genuchten, 1985; Sun et al., 1999a; Slodička and Balážová, 2008; Srinivasan and Clement, 2008). However, fission products, including xenon isotopes, can be formed directly (as independent yields or initial conditions) from fissions and through successive chain reactions (Saey et al., 2010). As shown in Fig. 1, xenon production involves multi-parent converging and multi-daughter branching reactions (Sun and Clement, 1999; Sun et al., 1999b; Lu et al., 2003; Sun et al., 2004; Yuan and Kernan, 2007). While parent species may be assumed to stay in solid or the liquid phase remaining well-contained in the chimney (Carrigan and Sun, 2012), xenon isotopes will be produced and transported in the gas phase from a detonation point to the ground surface. Therefore, xenon isotopes or their daughter products can be sampled in principle at or near the ground surface for discrimination purposes.

Using a batch-reactor model, the ordinary differential equations of the first-order reactions have been solved either analytically (e.g., Sun et al., 1999a, 2012) or numerically (e.g., Kalinowski et al., 2010; Kalinowski, 2011) and the resulting solution of the first-order chain reactions has been further used to calculate the Multi-Isotope Ratio Chart (MIRC, Kalinowski et al., 2010) used in discriminating between an underground nuclear explosion (UNE) and a civilian application. Because of the stiffness of ordinary differential equations involving a large difference (e.g., 6-orders of magnitude) in decay rates, additional numerical effort is required to meet convergence standards (Radhakrishnan and Hindmarsh, 1993). To avoid an extra computational expense for dealing with possible stiff reactions, closed-form solutions are preferred. In addition, closed-form solutions are required for the verification of numerical codes, which can be utilized in solving more complex, practical problems.

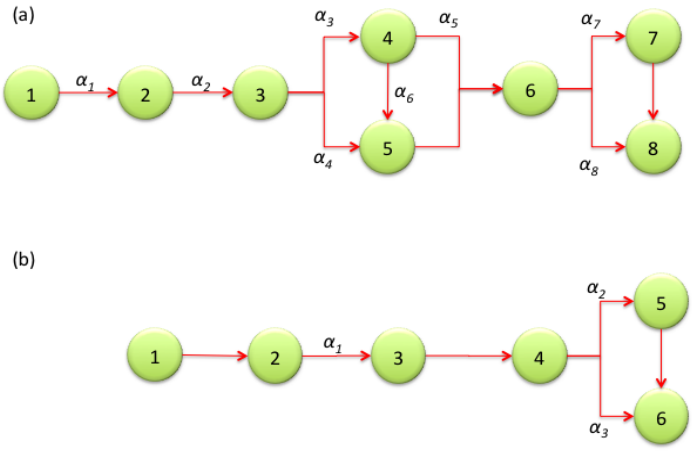

Figure 1. Reaction networks of (a) 131, 133, and (b) 135 isotopes. Reaction structure, independent fission yields, and decay branching factors are referred to England and Rider (1994). Isotopes, $i = 1,\ 2,\ \cdots,\ 8$ in (a), represent In, Sn, Sr, Te-m, Te, I, Xe-m, and Xe. Isotopes, $i = 1,\ 2,\ \cdots,\ 6$ in (b), represent Sn, Sr, Te, I, Xe-m, and Xe. α is branching factor. For the simplicity of mathematical formulation of reaction matrices and model development, isotopes are labeled by numbers.

Several numerical computer codes have been developed in the past for modeling reactive transport in geological systems (e.g., Nitao, 1998; Xu et al., 1998; Clement et al., 1998). A wide range of kinetic reactions at various time scales and equilibrium reactions are coupled with partial differential equations of multiphase flow and transport (Sun et al., 1998). Those reactive-transport codes have been mostly used for predicting liquid-phase concentrations. Nitao (1998) developed the capability of chain-reaction kinetics with multiphase flow and transport in NUFT code (see also Hao et al., 2012). Lowrey et al. (2012; 2013) used UTEX, a finite-difference code for modeling single-gas phase transport of xenon isotopes in a single fracture with chain reactions. Sun and Carrigan (2012) developed a numerical model of multiphase flow and transport in a realistic system with thermally-driven advection, barometric pumping, and diffusion, but without chain-reaction yields, that is, only the instantaneous, independent yield was considered.

In this paper, we develop a numerical modeling capability for simulating multiphase transport of noble gas radionuclides assuming fully coupled decay-chain networks with branching and converging reactions. Due to the lack of corresponding closed-form solutions for validating the numerical model and verifying the NUFT code, we further derive closed-form solutions for xenon-chain reactions in a batch reactor as well as for reactive transport in a 1-D column. In addition, we verify numerical solutions of chain reactions (Kalinowski, 2011; Nitao, 1998) in the absence of transport processes. Using the NUFT code, a numerical model is developed for studying multiphase flow and reactive transport and examining the Multi-Isotope Ratio Chart as a function of space and time for a geohydrologic regime of an actual UNE.

2. Methods

The mathematical model of radioxenon production and transport must be solved either directly through analytical means or by employing numerical methods. In this section, we derive an analytical

solution of the Xe-131m, -133m, -133, and -135 first-order reactions using analytical singular-value decomposition, and introduce the NUFT capability for fully coupled reaction kinetics coupled with multiphase transport. The analytical-solution scheme is also applied to derive a closed-form solution of xenon-chain reactive transport in a one-dimensional column for verifying the capability in NUFT.

2.1. Analytical Solution

The rate of change in radionuclide concentrations through a decay network can be expressed as (Sun et al., 2012)

$$\frac{d\mathbf{c}}{dt} = \mathbf{A}\mathbf{c} \tag{1}$$

where $\mathbf{A}$ [s^{-1}] is the first-order reaction matrix defined by the reaction network architecture, branching factors, and reaction rates, and $\mathbf{c}$ [mol m^{-3}] is the vector of concentrations. The solution of Eq. (1) can be symbolically expressed in an exponential form, $\mathbf{c} = \mathbf{c}^o \exp[-\mathbf{A}t]$, where $\mathbf{c}^o$ [mol m^{-3}] is the vector of initial concentrations and t [s] is time. The concentration vector mainly relies on the evaluation of the exponential matrix (Moler and van Loan, 1978; Moral and Pacheco, 2003).

Since both 131 and 133 networks are assumed to share the same reaction structure as shown in Figure 1a, the first-order reaction matrix $\mathbf{A}$ of 131 and 133 networks is expressed as

$$\mathbf{A} = \begin{bmatrix} -k_1 & 0 & 0 & 0 & 0 & 0 & 0 & 0 \\ \alpha_1 k_1 & -k_2 & 0 & 0 & 0 & 0 & 0 & 0 \\ 0 & \alpha_2 k_2 & -k_3 & 0 & 0 & 0 & 0 & 0 \\ 0 & 0 & \alpha_3 k_3 & -k_4 & 0 & 0 & 0 & 0 \\ 0 & 0 & \alpha_4 k_3 & \alpha_6 k_4 & -k_5 & 0 & 0 & 0 \\ 0 & 0 & 0 & \alpha_5 k_4 & k_5 & -k_6 & 0 & 0 \\ 0 & 0 & 0 & 0 & 0 & \alpha_7 k_6 & -k_7 & 0 \\ 0 & 0 & 0 & 0 & 0 & \alpha_8 k_6 & k_7 & -k_8 \end{bmatrix} \tag{2}$$

and reaction matrix of 135 chain is

$$\mathbf{A} = \begin{bmatrix} -k_1 & 0 & 0 & 0 & 0 & \\ k_1 & -k_2 & 0 & 0 & 0 & 0 \\ 0 & \alpha_1 k_2 & -k_3 & 0 & 0 & 0 \\ 0 & 0 & k_3 & -k_4 & 0 & 0 \\ 0 & 0 & 0 & \alpha_2 k_4 & -k_5 & 0 \\ 0 & 0 & 0 & \alpha_3 k_4 & k_5 & -k_6 \end{bmatrix}. \tag{3}$$

In Eqs. (2) and (3), $k = \ln(2)/t_{1/2}$ [s^{-1}] is the first-order reaction rate, $t_{1/2}$ [s] is the half-life time, α denotes branching factor (yield coefficient). Although Eq. (1) can be solved numerically (Clement et al., 1998; Kalinowski, 2011), closed-form solutions for 131, 133, and 135 reaction networks are derived for evaluating xenon production from nuclear detonations. Using the analytical singular-value decomposition (Sun et al., 2012), the reaction matrix $\mathbf{A}$ is analytically described as $\mathbf{A} = \mathbf{S}\mathbf{\Lambda}\mathbf{S}^-$, where $\mathbf{\Lambda}$ is an $M \times M$ diagonal matrix containing the eigenvalues of $\mathbf{A}$, $\mathbf{S}$ is a matrix whose columns are linearly independent eigenvectors of $\mathbf{A}$, $\mathbf{S}^-$ is the inverse matrix of $\mathbf{S}$, and the diagonal components of $\mathbf{\Lambda}$ are the exact reaction rates of the isotopes. Then, concentrations of all isotopes can be expressed analytically by using the closed-form expression of $\mathbf{S}$ and $\mathbf{S}^-$.

$\mathbf{S}^-$ and $\mathbf{S}$ called transformation matrices between the concentration domain and the transformed domain are expressed analytically as finite products of fractions of the form (Sun et al., 2012)

$$S^-_{i,j} = \sum_{\zeta=1}^{B_{i,j}} \left[\alpha_\zeta \prod_{l=1}^{n_{i,j}} \frac{k_{m(l)}}{k_{m(l)} - k_i} \right] \tag{4}$$

$$S_{i,j} = \sum_{\zeta=1}^{B_{i,j}} \left[\alpha_\zeta \frac{k_j}{k_i - k_j} \prod_{l=1}^{n_{i,j}-1} \frac{k_{m(l)}}{k_{m(l)} - k_j} \right] \tag{5}$$

where i is the current species index and j is an ancestor of species i, $m(l)$ is the species index of lth ancestor of i, and $n_{i,j}$ is the generation gap between species j and i, ζ is the branch number index, α_ζ is branching factor, $B_{i,j}$ is the number of branches to connect species i and j. If j is not an ancestor of i, $S^-_{i,j}$ and $S_{i,j}$ are defined to be zero. $S^-_{i,j} = S_{i,j} = 1$ when $i = j$.

The transformation matrices of 131, 133, and 135 reaction networks are derived and explicitly expressed in Appendices A and B. As illustrated by Sun et al. (2008; 2012), once the analytical form of $\mathbf{S}$ and $\mathbf{S}^-$ is derived, the singular-value decomposition can be applied to derive analytical solutions of $\mathbf{c}$. If an analytical solution of a single-species transport coupled with first-order reaction is available, the closed-form solution of all species concentrations in the fully coupled xenon reaction network is derived using (4) and (5). Except for the unique formulation of $\mathbf{S}$ and $\mathbf{S}^-$ for xenon reactions, the mathematical manipulation can be referred to Sun et al. (2008). The analytical solutions of chain reactions and one-dimensional chain-reactive transport are coded in MATLAB (MathWorks, 2000).

2.2. Numerical Solution

The USNT module of the NUFT computer code (Nitao, 1998; Hao et al., 2012) developed at Lawrence Livermore National Laboratory, is used to simulate multiphase and multi-species transport coupled with radioactive decay networks under non-isothermal conditions. Detailed description of the partial-differential equations is given by Hao et al. (2012). The generalized formulation of reaction kinetics fully coupled with mass- and energy-balance equations in the USNT module is expressed (Hao et al., 2012; Sun et al., 2012) as

$$\frac{d\omega_i}{dt} = \mu_i \exp\left[\frac{E}{RT_0} - \frac{E}{RT}\right] \prod_{j=1}^{M} \left(\omega_j^{a_j} \cdot \frac{\omega_j}{s_j + \omega_j} \cdot \frac{b_j}{b_j + \omega_j} \right), \; i = 1,\ 2, \cdots,\ N \tag{6}$$

where r_i [mol kg^{-1} s^{-1}] represents the molar-based reaction rate of reaction i, μ [mol kg^{-1} s^{-1}] is the maximum (contaminant) utilization rate, ω [-] is mole fraction, N [-] is the number of reactions, T [K] is the temperature, T_0 [K] is the reference temperature, s [kg kg^{-1}] is the saturation constant, R [J mol^{-1}K^{-1}] is the gas constant, E [J mol^{-1}] is the activation energy, a [-] is an exponent, and b [kg kg^{-1}] is the inhibition constant. The maximum utilization rate μ_i is expressed as a linear function of mass-based k_i [s^{-1}] or half life $t_{1/2}$ [s]

$$\mu_i = \frac{k_i}{\mathcal{M}_i} = -\frac{\ln 2}{\mathcal{M}_i t_{1/2,i}}, \quad i = 1,\ 2, \cdots,\ N \tag{7}$$

where $\mathcal{M}_i$ [kg mol^{-1}] is the molecular mass of species i.

Assuming temperature-independent radioactive decay with a_i=1, s_i=0, and b_i=1.0×10^{30}, the generalized kinetics is simplified as the first-order xenon reactions

$$\frac{d\omega_i}{dt} = -\frac{\ln 2}{\mathcal{M}_i t_{1/2,i}} \omega_i = \mu_i \omega_i. \tag{8}$$

A decay chain (Fig. 1) is represented by N connected reactions. The stoichiometric equation for reaction i, for example, is expressed

$$\omega_i \xrightarrow{\mu_i} \sum_{\zeta=1}^{B_i} \alpha_\zeta \omega_\zeta \tag{9}$$

where B_i is the number of branches for reaction i.

3. Model Validation and Code Verification

There is always a tradeoff between computational expense and model complexity. A summary of relevant computer models and representative solutions is provided in Table 1. To justify the procedure in Sect. 2.1 and Sect. 2.2, we conduct validation and verification in the following steps

1. Use MATLAB ode23s (MathWorks, 2000) to verify the analytical solution of xenon-chain reaction in a batch reactor in Sect. 2.1.
2. Use the analytical singular-value decomposition to derive an analytical solution of single-gas phase and xenon-chain transport in one-dimensional semi-infinite column.
3. Compare the NUFT results against the derived analytical solution in a batch reactor without considering transport.
4. Compare the NUFT results against the derived analytical solution with single-gas transport in a 1-D column.

Table 1. Computer models and solutions.

Dimension	Transport	Reaction	Analytical	Numerical
0D	Batch	Single-species	Exponential function	ODE
		Sequential-chain	Bateman (1910)	ODEs
		Xenon chain	**Sect. 2.1**	ode23s
1D	Liquid	Single-species	Bear (1979), P268	Nitao (1998)
	Liquid	Sequential-chain	Sun et al. (1999a)	Clement et al. (1998)
	Liquid	Complex chain	Sun et al. (2012)	Sun et al. (2008)
	Gas	Xenon chain	**Sect. 2.1**	**Sect. 2.2**
2D vertical fracture	Liquid	Sequential chain	Sun and Buscheck (2003)	Nitao (1998)
	Gas	Single species	-	Carrigan et al. (1996)
	Gas	Complex chain	-	Lowrey et al. (2012)
3D	Multiphase	Complex chain	-	**Sect. 2.2**

The justification of selected physical processes is referred to Sun and Carrigan (2012). Parameters used in the validation and verification are listed in Tables 2 and 3.

Table 2. Isotopes and half lives of xenon-reaction chain members.

Isotope	Index	131		133		Index	135	
In	1	0.282	[second]	0.180	[second]			
Sn	2	39.00	[second]	1.45	[second]	1	0.418	[second]
Sb	3	23.03	[minute]	2.5	[minute]	2	1.71	[second]
^{m}Te	4	30.0	[hour]	55.4	[minute]			
Te	5	25.0	[minute]	12.5	[minute]	3	19.0	[second]
I	6	8.0207	[day]	20.8	[hour]	4	6.57	[hour]
^{m}Xe	7	11.84	[day]	2.19	[day]	5	15.29	[minute]
Xe	8	Stable	[-]	5.243	[day]	6	9.14	[hour]

Data source: England and Rider (1994).

Table 3. Branching factors of xenon chain reactions (Fig. 1).

Reaction	Symbol	England		Saey		Symbol	England	Saey
		131	133	131	133		135	135
In→Sn	α_1	0.982	1.000	1.000	1.000	-	1.000	1.000
Sn→Sb	α_2	1.000	0.997	1.000	1.000	-	1.000	1.000
Sb→^{m}Te	α_3	0.070	0.420	0.090	0.170	-	0.000	0.000
Sb→Te	α_4	0.930	0.580	0.910	0.830	α_1	0.821	1.000
^{m}Te→I	α_5	0.820	0.870	0.778	0.700	-	0.000	0.000
^{m}Te→Te	α_6	0.180	0.130	0.222	0.175	-	0.000	0.000
I→^{m}Xe	α_7	0.014	0.028	0.012	0.029	α_2	0.147	0.168
I→Xe	α_8	0.986	0.972	0.988	0.971	α_3	0.853	0.834

England: England and Rider (1994). Saey: Saey et al. (2010).

3.1. Verification of Closed-Form Solution

For the sake of speed, efficiency, and accuracy, the analytical solution is preferred to directly calculate radioxenon activities as well as for verifying the numerical computer code. Before doing so, it is necessary to verify if the analytical solution is derived and implemented correctly. Following Kalinowski (2011), full chain reactions of Xe-131,-133, and -135 series, with all possible branching and converging connections, are expressed by ordinary differential equations and solved numerically using the MATLAB Rosenbrock method (ode23s). Using independent yields and the reaction architecture of the 131 chain (Fig. 1a) assuming a 1 kt ^{235f}U explosion (England and Rider, 1994), with the half lives (Table 2) and branching factors (Table 3, England and Rider, 1994), the time-dependent inventory of chain members is calculated as a function of time and compared as shown in Fig. 2.

Further applying the analytical and MATLAB numerical solutions for the 133 and 135 series, the ratio correlation is calculated and compared in Fig. 3. While the analytical solution of the xenon-isotopic ratio correlation is in excellent agreement with Kalinowski's (2011) numerical solution, the former has the advantage of not depending on the degree of convergence.

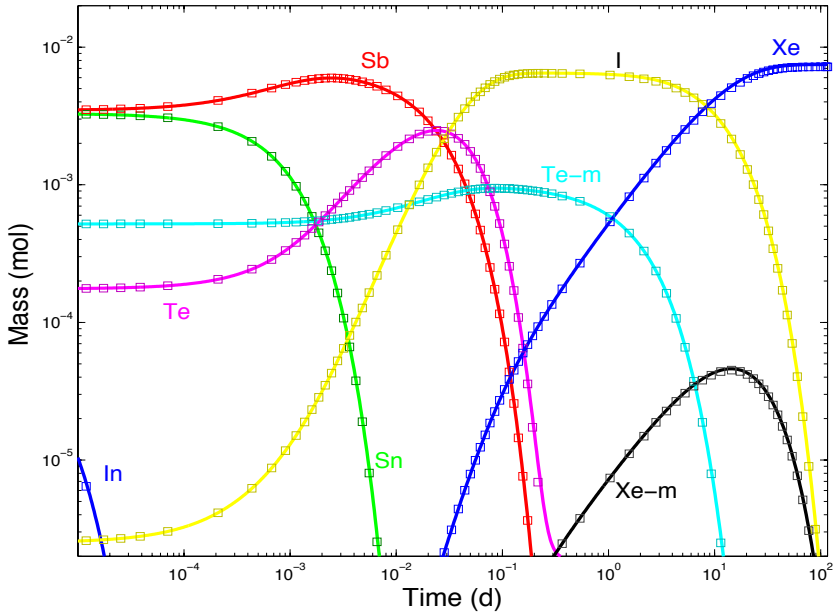

Figure 2. Comparison of mass profiles of 131 chain members calculated using analytical solution (solid lines) and numerical results (squares) obtained using MATLAB ode23s for 1kt ^{235f}U fission.

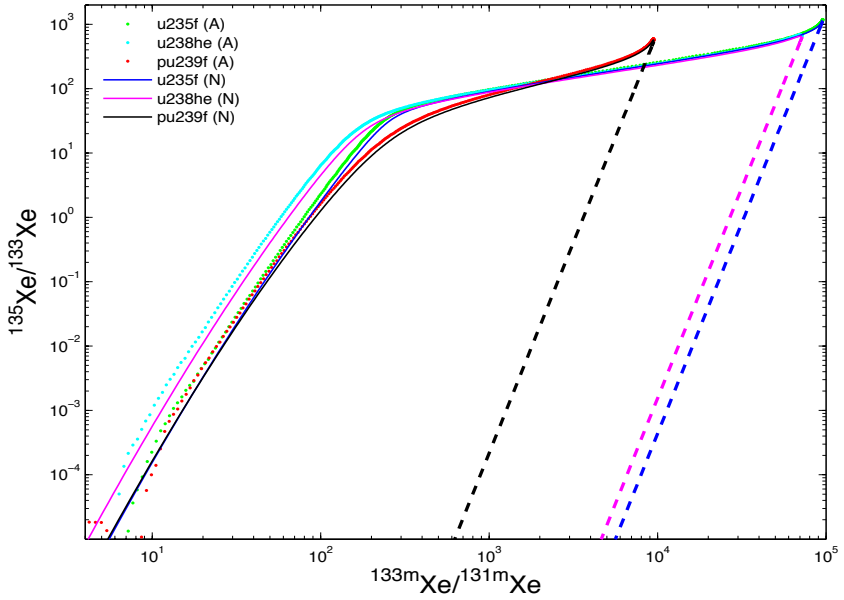

Figure 3. Comparison of xenon-isotopic-ratio correlations calculated using analytical solution (solid lines) and numerical results (dots) using MATLAB ode23s. The dashed lines represent the pure decay scenarios without considering ingrowth. (A) and (N) denote analytical and numerical solutions, respectively. Note that four xenon isotopes from three fission types were chosen to match Kalinowski et al. (2010).

3.2. Verification of NUFT

Taking the 131 reaction network (i.e., decay chain with branching and convergence) (Fig. 1a) as an example, the kinetic reaction module of NUFT is verified by comparing numerical results against the derived analytical solution. To check the reaction package alone, transport processes are modeled with zero values of velocity, diffusivity, and dispersivity. Initial concentrations of all daughter species are assumed to be zero while the initial concentration of In-131 is assumed to be 1. The CPU time required for running the NUFT model is 27000 times greater than that required for evaluating the analytical solution. As shown in Fig. 4, the solution can be considered identical although the numerical solution requires much more CPU time.

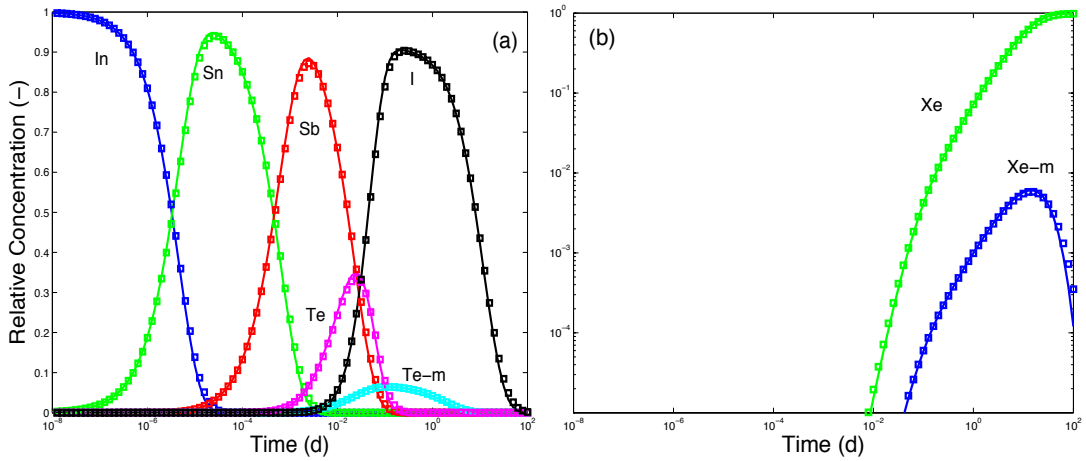

Figure 4. Comparison of analytical and numerical solutions of Xe-131 chain reactions in a batch reactor. (a) Concentrations of In-131, Sn-131, Sb-131, Te-131m, Te-131, and I-131. (b) Concentrations of Xe-131m and Xe-131. Solid lines and squares represent analytical and numerical solutions, respectively.

The analytical transformation matrices, Eqs. (4) and (5), are further used to formulate the analytical solution of transport coupled with radioactive decay networks. Using the same 131 reaction network, the numerical simulation of single-gas transport in a semi-infinite column is compared against the analytical solution in Fig. 5. Evaluation of the 1-D transport solution in this case is done analytically in about 1/3000 of the time required to obtain the numerical result. The formulation of the analytical solution is referred to Sun et al. (2012) with unique transformation matrices provided in Appendix A. For the availability of analytical solutions, flow velocity, diffusivity, and dispersivity are assumed to be the same and constant for all chain members.

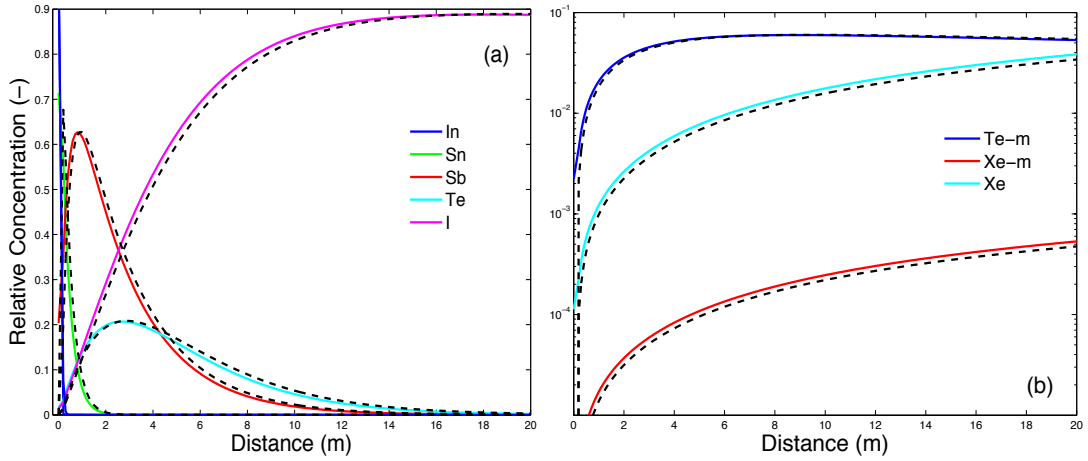

Figure 5. Comparison of analytical and numerical solutions of Xe-131 reactive transport in a one-dimensional column at 50 days. (a) Concentrations of In-131, Sn-131, Sb-131, Te-131, and I-131. (b) Concentrations of Te-131m, Xe-131m, and Xe-131. Solid and dashed lines represent analytical and numerical solutions, respectively. Dispersivity and velocity are assumed to be 5.0 m and 4.18×10^{-4} m s^{-1}.

4. Results and Analyses

In this section, we present numerical results from models of (1) xenon-decay reaction in a batch reactor corresponding to Kalinowski (2011), (2) xenon-reactive transport in a vertical fracture corresponding to Lowrey et al. (2012), and (3) xenon reactive transport under non-isothermal conditions in the Test Bed #1 system.

4.1. Xenon Production in A Batch Reactor

In the absence of transport, the numerical solution of xenon-chain reactions represents source-term inventory of radionuclides as a function of time. Fig. 6 shows radioactivities of iodine and xenon isotopes from 1 kt ^{235f}U detonation.

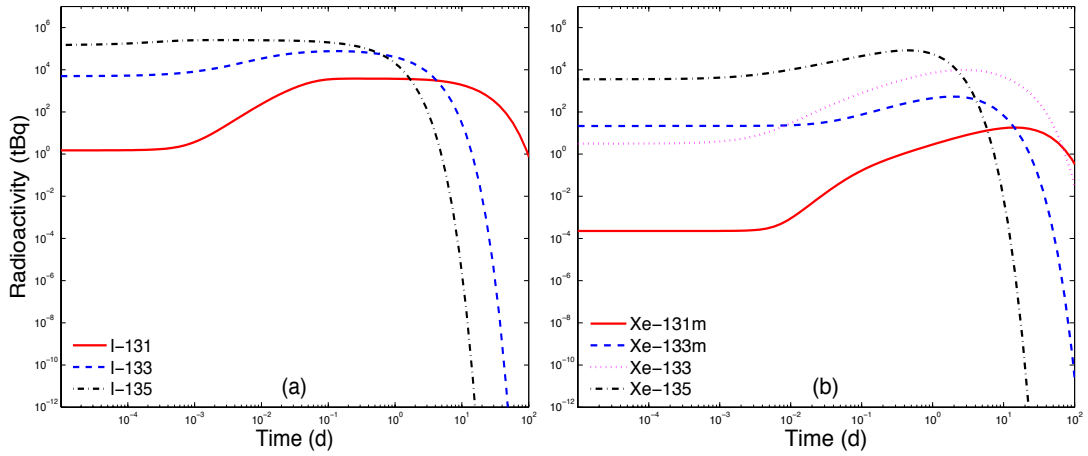

Figure 6. Radioactivities of (a) iodine and (b) xenon isotopes for 1kt ^{235f}U fission.

Fig. 7 shows isotopic ratio correlations for the three fissioning types of Fig. 8 of Kalinowski et al. (2010). Since gas concentrations are mainly determined by linear physical processes, such as advection, diffusion, dispersion, and first-order reactions, a meaningful log-log correlation (e.g., Fig. 7) of xenon isotopic ratios at low values of the isotopic ratios requires that the values of individual concentrations be measured very accurately. Fig. 7 is also plotted on linear and semi-log scale as shown in Fig. 8. These alternative approaches to plotting the Kalinowski MIRC show that small values of isotopic ratios resulting from a UNE will tend to fall so close to the discrimination line (red-dashed line) that small errors or noise in making a ratio determination have the potential to affect the interpretation of a particular data point as to whether or not it results from a UNE.

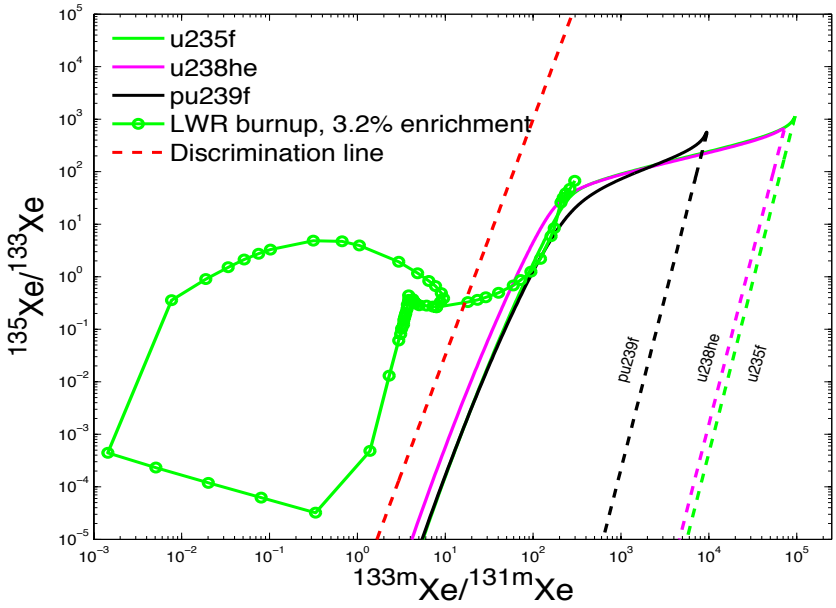

Figure 7. Isotopic ratio correlation of of ^{235f}U, ^{238he}U, and ^{239f}Pu (see Fig. 8 of Kalinowski et al., 2010). The red dotted line is the discrimination line. The green curve of xenon isotopic rations of light-water reactor is plotted as a reference (Kalinowski and Pistner, 2006).

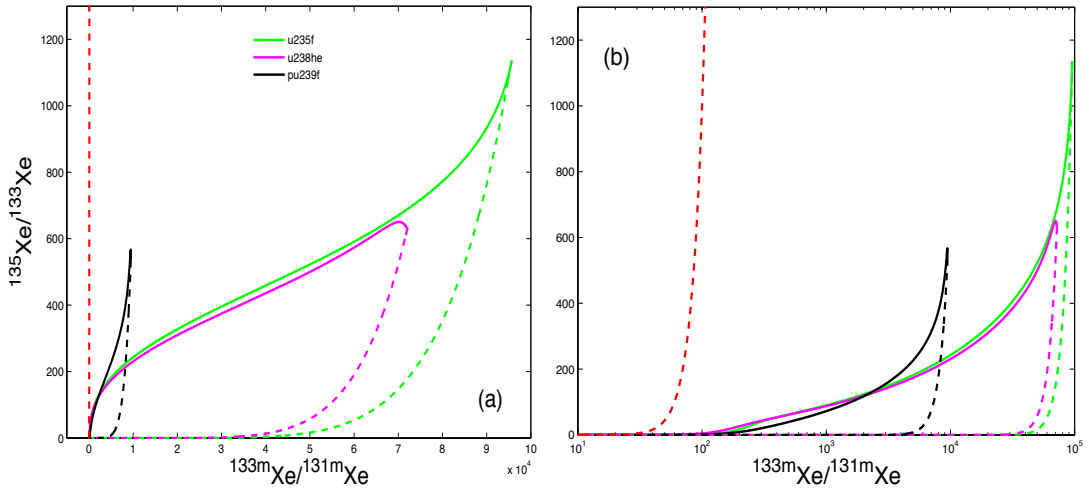

Figure 8. Isotopic ratio correlation of three fission types of Kalinowski et al. (2010) on (a) linear-linear and (b) semi-log scales. The red dashed line is the discrimination line.

4.2. Xenon Production and Transport in a Vertical Fracture

In the NPE model (Carrigan et al., 1996; Sun and Carrigan, 2012, see Fig. 1b of Sun and Carrigan, 2012), barometric pumping and diffusion are considered as the driving force for gas transport from the *halo* to the ground surface without considering chain reactions. This model with a single vertical fracture cutting through the rock matrix is similar to that of Lowrey et al. (2012) except for the implicitly coupled reactions. Using the fully coupled reaction capability developed in NUFT, we modified the NPE model by implementing independent yields in the *halo* zone as an initial condition and allowing full chain reactions in the entire domain. This model assumes that the radionuclide inventory resulting from the detonation is effectively distributed throughout the *halo* zone. The corresponding isotopic ratio correlation is calculated and plotted in Fig. 9. While data points (purple line) at 200-m depth closely track the Kalinowski decay-ingrowth curve, the xenon isotopic ratio correlation at shallower 4-m and 100-m depths does not track the decay and ingrowth curve but do cross the discrimination line. Note that radioactivities of xenon isotopes simulated at the depth of 4 m are below the currently assumed measurable limit of 1 mBq m^{-3}. Even though the MIRC can be modeled theoretically, the chart may not be practical because of non-detectable levels of radioactivity or missing isotopes such as Xe-135 which appears to limit the applicability of a 4-isotope plot to about 10 days following an explosion.

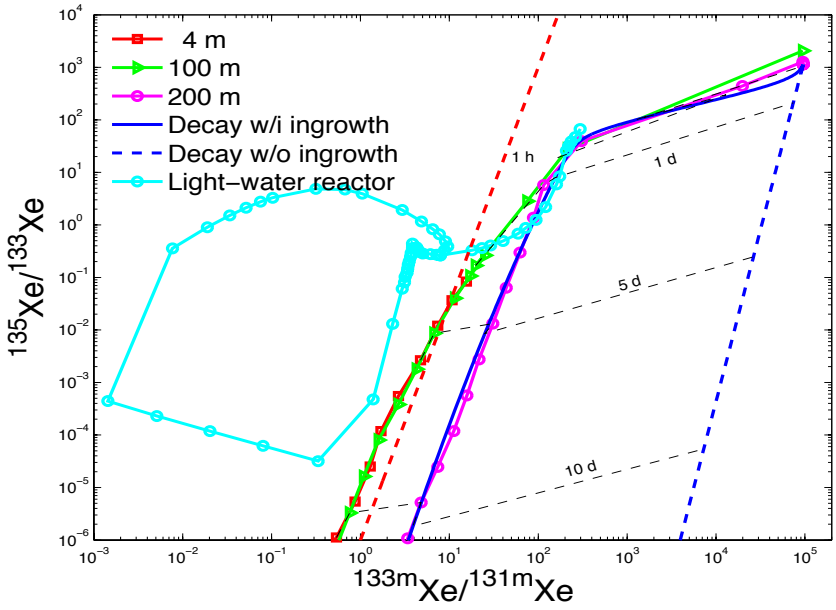

Figure 9. Isotopic-ratio correlation computed as a function of time and depth in the single-fracture NPE model for 1kt ^{235f}U detonation. Radioactivities simulated at the depth of 4 m are below the current measurable limit.

4.3. Xenon Production and Multiphase Transport

To further investigate the effect of multiphase transport with phase partitioning between gas and liquid, we developed a model for a hypothetical nuclear explosion at Test Bed #1. The flow and transport model is similar to the much simpler Rainier model of Sun and Carrigan (2012). This more

sophisticated model assumes a non-isothermal, two-phase flow with water and air as principal components as considered before, but instead of assuming the presence of three independent components (Xe-133, Ar-37, and SF_6), we now consider 22 chain-reaction members as minor components (Table 2) fully coupled with first-order reaction networks as shown in Fig. 1. The geological formation is described as a dual-permeability medium of overlapping fracture and matrix continua with an assumed geometry of the cavity, chimney, and altered zone. The physical system is discretized in a radially-symmetric (cylindrical) coordinate system.

Using this model, a series of numerical experiments were conducted allowing comparison of the roles of different transport processes on measured xenon isotopic concentrations. In the simulations, the spatial and temporal influence of isotopic migration by diffusion, barometric pumping, and thermally-induced advection caused by explosion-residual heat in the chimney was considered. The corresponding correlations of xenon isotopic ratios are plotted in Fig. 10 at 5-m depth and in the entire domain between 2.0 hours and 10 days.

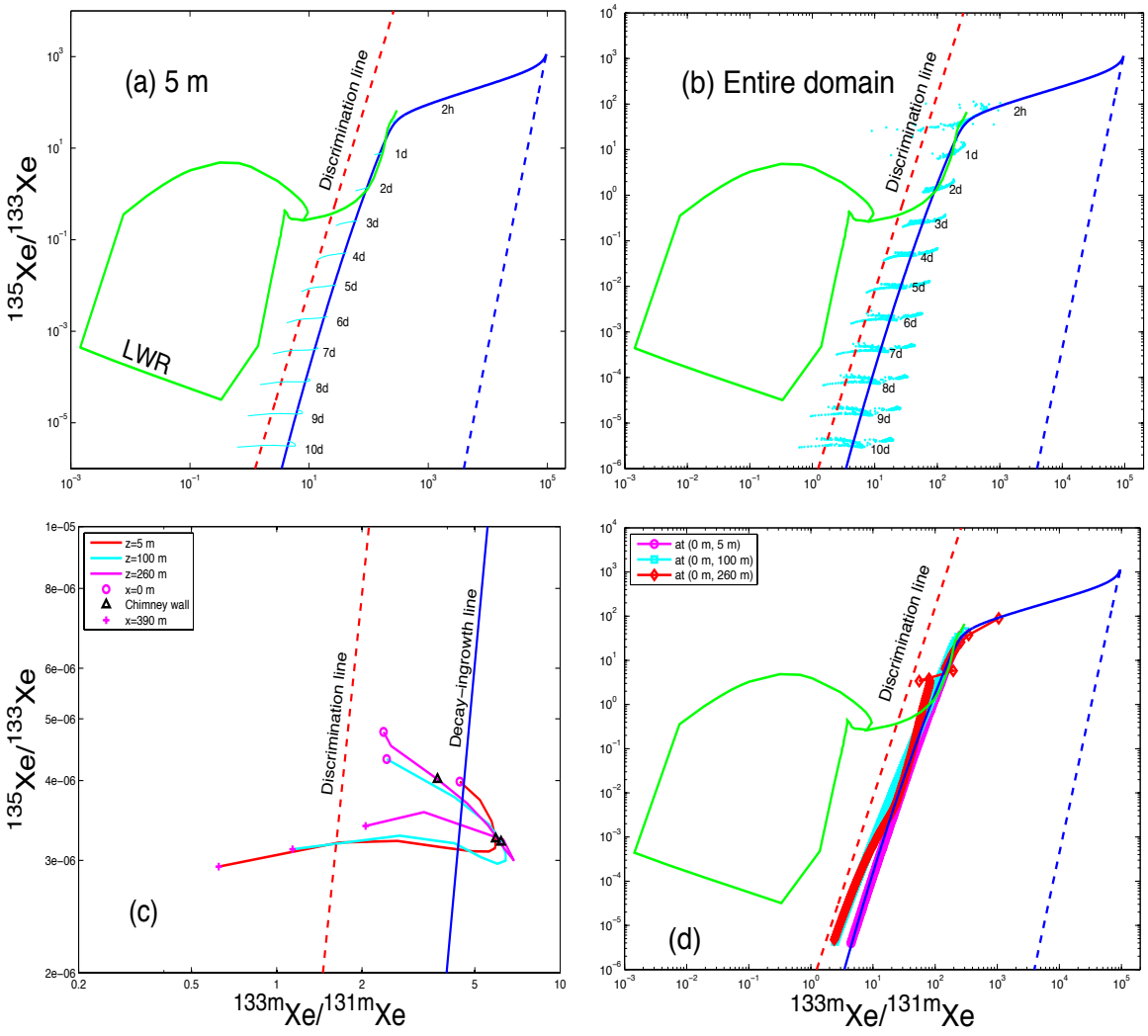

Figure 10. Isotopic ratio correlation of ^{235f}U detonation at Test Bed #1. (a) MIRC within the depth of 5 m at 11 time steps between 2.0 hours and 10 days. (b) MIRC in the entire domain for $z \in$[0, 660] m and $r \in$[0, 490] m at various times. (c) MIRC at 10 days as a function of radial distance between 0 and 390 m at depth of 5, 100, and 260 m, which represent near-surface, above chimney, and chimney conditions. (d) MIRC at (0, 5), (0, 100), and (0, 260) as functions of time.

We find that at early times (i.e., hours to days) to accurately quantify isotopic ratios of short-lived isotopes, such as ^{131m}Xe (11.93d), ^{133m}Xe (2.19d), ^{133}Xe (5.24d), and ^{135}Xe (9.10h), thermally-driven advection must be considered. Similar to the model results of the Rainier explosion (Sun and Carrigan, 2012), thermally-driven advection is the major physical process that delivers noble gases to the ground surface before the chimney temperature drops below the boiling point. With advection, four xenon isotopes reach the ground surface with radioactivities above 1 mBq m^{-3} at 2.0 hours. Without advection, ^{133m}Xe, never reaches the detection threshold at or near the ground surface.

Matrix diffusion buffers (retards) gas-phase release from underground explosions. Compared to the thermally-driven advection, diffusion is a less sensitive physical process for early-time detection. Long-lived and stable isotopes, such as ^{131}Xe and ^{135m}Xe, may also be delivered to the ground surface by barometric pumping in the post-boiling period.

Figure 10c shows the MIRC at 10 days as a function of radial distance at various depths for near-surface (5 m), above-chimney (100 m), and chimney conditions (260 m). This simulation suggests that the MIRC from a deep drill-back hole may cross over the discrimination line. It is also observed in Figure 10d that the MIRC at the depth of 260 m migrates across the line at about 7 days.

4.4. Effect of Branching Factors

To this point we have only considered the effect of different transport processes on influencing measurable xenon isotopic ratios at the surface. We also investigated the effect of uncertainties of isotopic half lives and network branching factors on the values of isotopic ratios that might be measured at the surface. We find that the uncertainty of isotopic half lives reported by England and Rider (1994) does not significantly affect the ratio values. In addition, two different sets of branching factors reported in the literature as listed in Table 3 slightly affect the ratios. Those factors, defined by α_ζ in Sect. 2.1, determine the transformation matrices $\mathbf{S}^-$ and $\mathbf{S}$ (Eqs. 4 and 5) and control the chain-reaction yields of daughter isotopes. To understand the effect of those factors on xenon production, we ran the analytical solution for three typical fissions in a batch reactor mode and produced the correlation of xenon isotopic ratios as shown in Fig. 11. The two curves agree well with each other on the log-log scale and (Fig. 11), even though the discrepancy in the calculation of the radioactivities can reach 16% on a linear scale as shown in Fig. 12. Thus, we do not consider either the current uncertainty in half lives or branching factors to be a major impediment to the practical simulation of xenon isotopic ratios as measured at the surface. Indeed, such uncertainties are small compared to the geo-hydrologic uncertainty present in the base model.

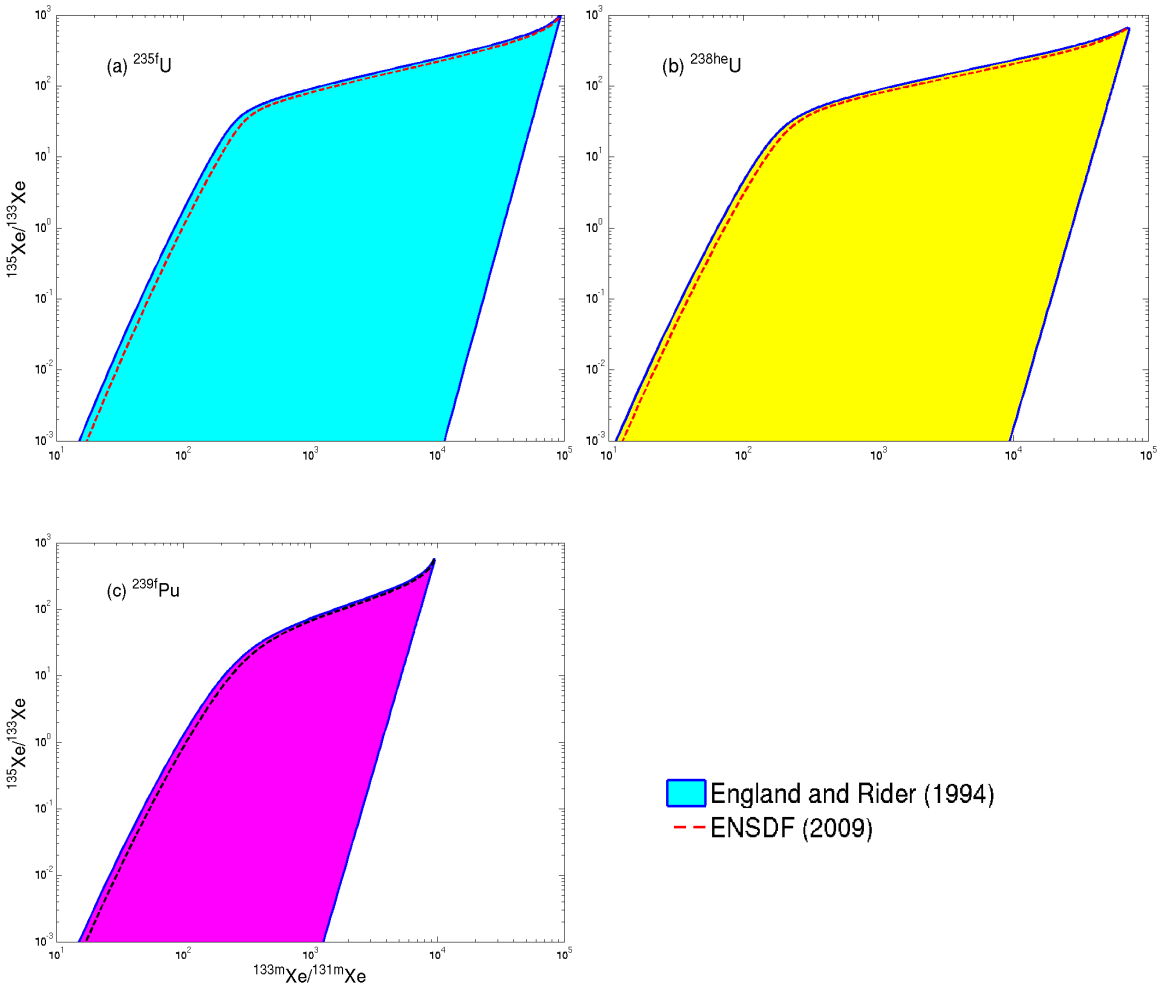

Figure 11. Comparison of xenon-isotopic ratio correlations on log-log scale using branching ratios from England and Rider (1994) and ENSDF (2009) for (a) ^{235f}U, (b) ^{238he}U, and (c) ^{239f}Pu. Note that the dashed curves represent results using ENSDF (2009) and the shaded area bounded with solid lines denotes the results using England and Rider (1994).

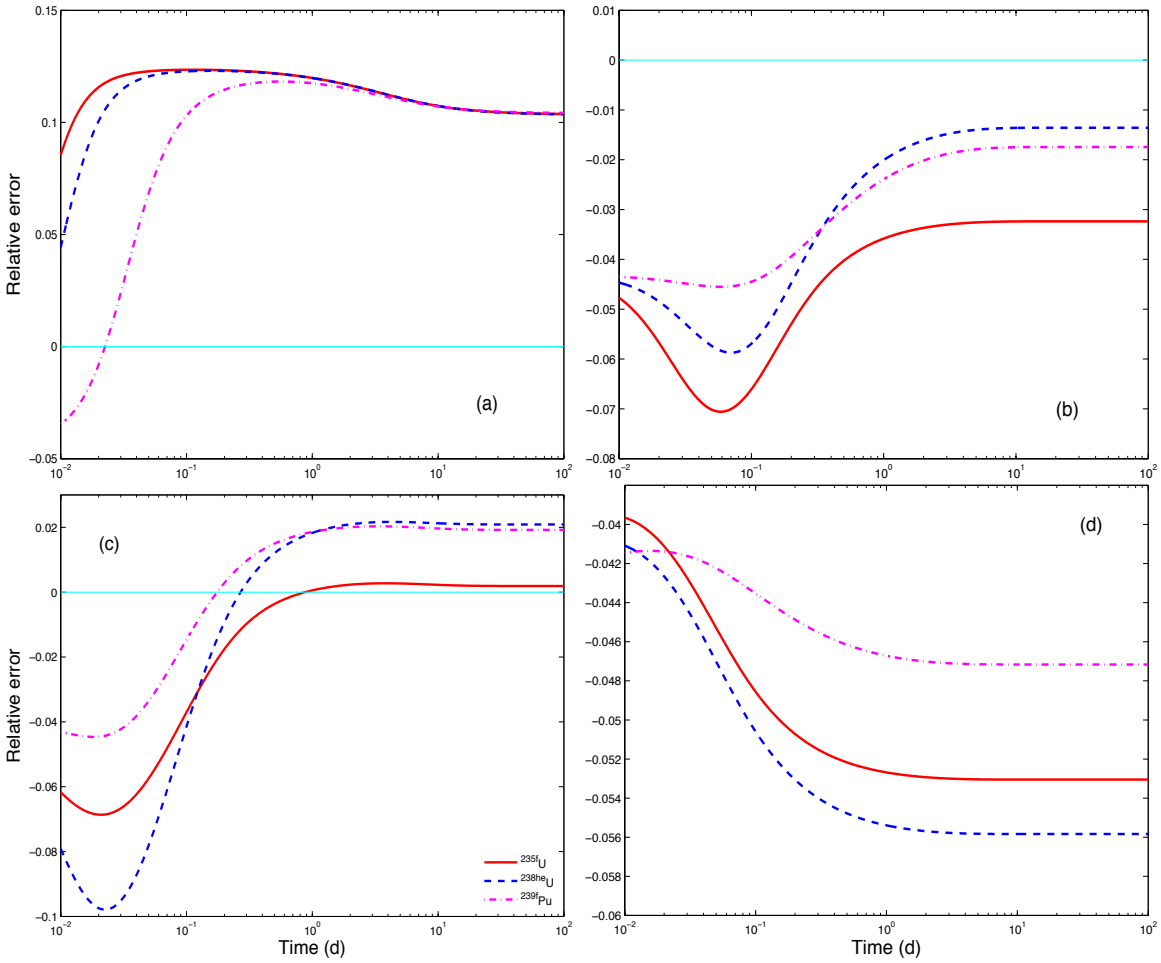

Figure 12. Relative difference in radioactivities of (a) Xe-131m, (b) Xe-133m, (c) Xe-133, and (d) Xe-135 between England and Rider (1994) and ENSDF (2009) branching factors.

5. Discussion and Conclusions

A computer model has been developed for studying radioxenon production from underground nuclear detonations and multiphase transport from the detonation point to the ground surface. To validate the model and verify the corresponding computer code, we derived analytical solutions of xenon chain reactions in a batch reactor mode and also single-gas phase transport coupled with chain reactions in a one-dimensional column. Calculations involving these analytical and numerical models were performed in this paper to gain the following key insights:

1. Isotopic-ratio correlation between Xe-133m/Xe-131m and Xe-135/Xe133, developed by Kalinowski et al. (2010), can be derived using analytical singular-value decomposition. The analytical solution derived avoids the additional effort of implementing stiff ode solvers and produces a time-dependent inventory of all chain decay members, as well as the isotopic-ratio correlations, at a much reduced computational cost.

2. An analytical solution of single-gas phase transport coupled with radioactive fission chain reactions was derived for verifying the numerical model and studying single-gas transport fully coupled with first-order chain reactions.

3. The numerical model of multiple-phase transport fully coupled with xenon-chain reactions is validated and verified to the extent possible. It can be used as a numerical laboratory for studying underground-explosion-relevant signals and their potential application to discriminating between UNE and civilian events.

4. Different branching factors, as shown in Fig. 1, were reported in the literature. The resulting discrepancy in modeled isotopic-ratio correlation looks insignificant on a log-log scale even though the relative error of modeled xenon radioactivities, at the ground surface of Test Bed #1, can be as high as 16%.

5. A model of single-gas-phase transport in a vertical fracture does not represent the transport driven by explosion residual heat. As indicated by Sun and Carrigan (2012), the thermally driven advection and phase change are the major force to deliver noble gases to the ground surface at early times. However, as the residual heat declines, barometric pumping becomes progressively more important for transporting long-life isotopes. Thermally driven advection is likely to be the principal mechanism responsible for transporting short-life isotopes to the surface in the days immediately following a well-contained UNE. To facilitate further comparison of the relationship between IMS and OSI isotopic measurements, the subsurface transport model fully coupled with chain reactions can serve as a source in both IMS large-scale atmospheric and OSI subsurface models.

6. The effect of geological uncertainties (structure and parametric) on xenon isotopic activities at the ground surface is significant. Further uncertainty quantification is needed for evaluating model predictability and reliability.

7. The Kalinowski MIRC appears to be highly appropriate in its application to atmospheric gas releases from above-ground or poorly contained underground nuclear explosions. However, for more well-contained scenarios, such as the one investigated here, the simulated isotopic ratios as plotted on the MIRC are complicated due to gas mixing and transport which include the effects of subsurface chemical fractionation, time-dependent nuclide inventories, and dual-permeability fractured rock. In the simulations presented here, xenon isotopic ratios were found to be both temporally and spatially dependent. At some distances from surface ground zero, it was found that the ratios would cross the discrimination line depending on the depth at which the gas concentrations are evaluated. Because of the short half-life of Xe-135 (9.10 h), creating a 4-isotope MIRC may only be possible if the isotopes can be measured during the first few days following a UNE.

8. Finally, we find a somewhat counter-intuitive result when xenon isotopic ratios are plotted for different depths on a MIRC (Fig. 10c) since shallower depths appear to yield ratios that are clearly in the nuclear explosion domain while ratios calculated for greater depths, that is, closer to the detonation point, appear to produce ratios that can fall across the discrimination line into the civilian nuclear activity domain. This is a difficult result that demands more detailed consideration requiring additional modeling of the spatial isotopic distribution as a function of time.

Acknowledgements

The authors wish to thank Martin B. Kalinowski at Carl Friedrich von Weizsäcker Center for Science and Peace Research (ZNF) and Carol A. Velsko at Lawrence Livermore National Laboratory for providing and interpreting data of fission product decay chains. The authors also thank Nathan G. Wimer and Steven A. Kreek at Lawrence Livermore National Laboratory for their careful review and helpful comments that led to an improved manuscript. This research was funded by Office of Proliferation Detection (NA-221), U.S. Department of Energy and performed under the auspices of

the U.S. Department of Energy by Lawrence Livermore National Laboratory under Contract No. DE-AC52-07NA27344.

Appendix A: Transformation Matrices of 131 and 133 Decay Networks

Transformation matrices $\mathbf{S}^-$ and $\mathbf{S}$ of 131 and 133 decay networks are formulated as:

$$\mathbf{S}^- = \begin{bmatrix} 1 & 0 & 0 & 0 & 0 & 0 & 0 & 0 \\ \frac{\alpha_1 k_1}{k_1-k_2} & 1 & 0 & 0 & 0 & 0 & 0 & 0 \\ S^-_{3,1} & \frac{\alpha_2 k_2}{k_2-k_3} & 1 & 0 & 0 & 0 & 0 & 0 \\ S^-_{4,1} & S^-_{4,2} & \frac{\alpha_3 k_3}{k_3-k_4} & 1 & 0 & 0 & 0 & 0 \\ S^-_{5,1} & S^-_{5,2} & S^-_{5,3} & \frac{\alpha_6 k_4}{k_4-k_5} & 1 & 0 & 0 & 0 \\ S^-_{6,1} & S^-_{6,2} & S^-_{6,3} & S^-_{6,4} & \frac{k_5}{k_5-k_6} & 1 & 0 & 0 \\ S^-_{7,1} & S^-_{7,2} & S^-_{7,3} & S^-_{7,4} & S^-_{7,5} & \frac{\alpha_7 k_6}{k_6-k_7} & 1 & 0 \\ S^-_{8,1} & S^-_{8,2} & S^-_{8,3} & S^-_{8,4} & S^-_{8,5} & S^-_{8,6} & \frac{k_7}{k_7-k_8} & 1 \end{bmatrix} \tag{10}$$

where

$$\begin{aligned}
S^-_{3,1} &= \frac{\alpha_1 k_1}{k_1-k_3}\cdot\frac{\alpha_2 k_2}{k_2-k_3} \quad (1\ \overrightarrow{\alpha_1}\ 2\ \overrightarrow{\alpha_2}\ 3) \\
S^-_{4,1} &= \frac{\alpha_1 k_1}{k_1-k_4}\cdot\frac{\alpha_2 k_2}{k_2-k_4}\cdot\frac{\alpha_3 k_3}{k_3-k_4} \quad (1\ \overrightarrow{\alpha_1}\ 2\ \overrightarrow{\alpha_2}\ 3\ \overrightarrow{\alpha_3}\ 4) \\
S^-_{5,1} &= \frac{\alpha_1 k_1}{k_1-k_5}\cdot\frac{\alpha_2 k_2}{k_2-k_5}\cdot\frac{\alpha_3 k_3}{k_3-k_5}\cdot\frac{\alpha_6 k_4}{k_4-k_5} \quad (1\ \overrightarrow{\alpha_1}\ 2\ \overrightarrow{\alpha_2}\ 3\ \overrightarrow{\alpha_3}\ 4\ \overrightarrow{\alpha_6}\ 5) \\
&+ \frac{\alpha_1 k_1}{k_1-k_5}\cdot\frac{\alpha_2 k_2}{k_2-k_5}\cdot\frac{\alpha_4 k_3}{k_3-k_5} \quad (1\ \overrightarrow{\alpha_1}\ 2\ \overrightarrow{\alpha_2}\ 3\ \overrightarrow{\alpha_4}\ 5) \\
S^-_{6,1} &= \frac{\alpha_1 k_1}{k_1-k_6}\cdot\frac{\alpha_2 k_2}{k_2-k_6}\cdot\frac{\alpha_3 k_3}{k_3-k_6}\cdot\frac{\alpha_5 k_4}{k_4-k_6} \quad (1\ \overrightarrow{\alpha_1}\ 2\ \overrightarrow{\alpha_2}\ 3\ \overrightarrow{\alpha_3}\ 4\ \overrightarrow{\alpha_5}\ 6) \\
&+ \frac{\alpha_1 k_1}{k_1-k_6}\cdot\frac{\alpha_2 k_2}{k_2-k_6}\cdot\frac{\alpha_3 k_3}{k_3-k_6}\cdot\frac{\alpha_6 k_4}{k_4-k_6}\cdot\frac{k_5}{k_5-k_6} \quad (1\ \overrightarrow{\alpha_1}\ 2\ \overrightarrow{\alpha_2}\ 3\ \overrightarrow{\alpha_3}\ 4\ \overrightarrow{\alpha_6}\ 5\to 6) \\
&+ \frac{\alpha_1 k_1}{k_1-k_6}\cdot\frac{\alpha_2 k_2}{k_2-k_6}\cdot\frac{\alpha_4 k_3}{k_3-k_6}\cdot\frac{k_5}{k_5-k_6} \quad (1\ \overrightarrow{\alpha_1}\ 2\ \overrightarrow{\alpha_2}\ 3\ \overrightarrow{\alpha_4}\ 5\to 6) \\
S^-_{7,1} &= \frac{\alpha_1 k_1}{k_1-k_7}\cdot\frac{\alpha_2 k_2}{k_2-k_7}\cdot\frac{\alpha_3 k_3}{k_3-k_7}\cdot\frac{\alpha_5 k_4}{k_4-k_7}\cdot\frac{\alpha_7 k_6}{k_6-k_7} \quad (1\ \overrightarrow{\alpha_1}\ 2\ \overrightarrow{\alpha_2}\ 3\ \overrightarrow{\alpha_3}\ 4\ \overrightarrow{\alpha_5}\ 6\ \overrightarrow{\alpha_7}7) \\
&+ \frac{\alpha_1 k_1}{k_1-k_7}\cdot\frac{\alpha_2 k_2}{k_2-k_7}\cdot\frac{\alpha_3 k_3}{k_3-k_7}\cdot\frac{\alpha_6 k_4}{k_4-k_7}\cdot\frac{k_5}{k_5-k_7}\cdot\frac{\alpha_7 k_6}{k_6-k_7} \quad (1\ \overrightarrow{\alpha_1}\ 2\ \overrightarrow{\alpha_2}\ 3\ \overrightarrow{\alpha_3}\ 4\ \overrightarrow{\alpha_6}\ 5\to 6\ \overrightarrow{\alpha_7}\ 7) \\
&+ \frac{\alpha_1 k_1}{k_1-k_7}\cdot\frac{\alpha_2 k_2}{k_2-k_7}\cdot\frac{\alpha_4 k_3}{k_3-k_7}\cdot\frac{k_5}{k_5-k_7}\cdot\frac{\alpha_7 k_6}{k_6-k_7} \quad (1\ \overrightarrow{\alpha_1}\ 2\ \overrightarrow{\alpha_2}\ 3\ \overrightarrow{\alpha_4}\ 5\to 6\ \overrightarrow{\alpha_7}\ 7) \\
S^-_{8,1} &= \frac{\alpha_1 k_1}{k_1-k_8}\cdot\frac{\alpha_2 k_2}{k_2-k_8}\cdot\frac{\alpha_3 k_3}{k_3-k_8}\cdot\frac{\alpha_5 k_4}{k_4-k_8}\cdot\frac{\alpha_7 k_6}{k_6-k_8}\cdot\frac{k_7}{k_7-k_8} \quad (1\ \overrightarrow{\alpha_1}\ 2\ \overrightarrow{\alpha_2}\ 3\ \overrightarrow{\alpha_3}\ 4\ \overrightarrow{\alpha_5}\ 6\ \overrightarrow{\alpha_7}\ 7\to 8) \\
&+ \frac{\alpha_1 k_1}{k_1-k_8}\cdot\frac{\alpha_2 k_2}{k_2-k_8}\cdot\frac{\alpha_3 k_3}{k_3-k_8}\cdot\frac{\alpha_5 k_4}{k_4-k_8}\cdot\frac{\alpha_8 k_6}{k_6-k_8} \quad (1\ \overrightarrow{\alpha_1}\ 2\ \overrightarrow{\alpha_2}\ 3\ \overrightarrow{\alpha_3}\ 4\ \overrightarrow{\alpha_5}\ 6\ \overrightarrow{\alpha_8}\ 8) \\
&+ \frac{\alpha_1 k_1}{k_1-k_8}\cdot\frac{\alpha_2 k_2}{k_2-k_8}\cdot\frac{\alpha_3 k_3}{k_3-k_8}\cdot\frac{\alpha_6 k_4}{k_4-k_8}\cdot\frac{k_5}{k_5-k_8}\cdot\frac{\alpha_7 k_6}{k_6-k_8}\cdot\frac{k_7}{k_7-k_8} \quad (1\ \overrightarrow{\alpha_1}\ 2\ \overrightarrow{\alpha_2}\ 3\ \overrightarrow{\alpha_3}\ 4\ \overrightarrow{\alpha_6}\ 5\to 6\ \overrightarrow{\alpha_7}\ 7\to 8) \\
&+ \frac{\alpha_1 k_1}{k_1-k_8}\cdot\frac{\alpha_2 k_2}{k_2-k_8}\cdot\frac{\alpha_3 k_3}{k_3-k_8}\cdot\frac{\alpha_6 k_4}{k_4-k_8}\cdot\frac{k_5}{k_5-k_8}\cdot\frac{\alpha_8 k_6}{k_6-k_8} \quad (1\ \overrightarrow{\alpha_1}\ 2\ \overrightarrow{\alpha_2}\ 3\ \overrightarrow{\alpha_3}\ 4\ \overrightarrow{\alpha_6}\ 5\to 6\ \overrightarrow{\alpha_8}\ 8) \\
&+ \frac{\alpha_1 k_1}{k_1-k_8}\cdot\frac{\alpha_2 k_2}{k_2-k_8}\cdot\frac{\alpha_4 k_3}{k_3-k_8}\cdot\frac{k_5}{k_5-k_8}\cdot\frac{\alpha_7 k_6}{k_6-k_8}\cdot\frac{k_7}{k_7-k_8} \quad (1\ \overrightarrow{\alpha_1}\ 2\ \overrightarrow{\alpha_2}\ 3\ \overrightarrow{\alpha_4}\ 5\to 6\ \overrightarrow{\alpha_7}\ 7\to 8) \\
&+ \frac{\alpha_1 k_1}{k_1-k_8}\cdot\frac{\alpha_2 k_2}{k_2-k_8}\cdot\frac{\alpha_4 k_3}{k_3-k_8}\cdot\frac{k_5}{k_5-k_8}\cdot\frac{\alpha_8 k_6}{k_6-k_8} \quad (1\ \overrightarrow{\alpha_1}\ 2\ \overrightarrow{\alpha_2}\ 3\ \overrightarrow{\alpha_4}\ 5\to 6\ \overrightarrow{\alpha_8}\ 8)
\end{aligned}$$

$$
\begin{aligned}
S^{-}_{4,2} &= \frac{\alpha_2 k_2}{k_2-k_4}\cdot\frac{\alpha_3 k_3}{k_3-k_4} \quad (2\ \overrightarrow{\alpha_2}\ 3\ \overrightarrow{\alpha_3}\ 4)\\
S^{-}_{5,2} &= \frac{\alpha_2 k_2}{k_2-k_5}\cdot\frac{\alpha_3 k_3}{k_3-k_5}\cdot\frac{\alpha_6 k_4}{k_4-k_5} \quad (2\ \overrightarrow{\alpha_2}\ 3\ \overrightarrow{\alpha_3}\ 4\ \overrightarrow{\alpha_6}\ 5)\\
&+ \frac{\alpha_2 k_2}{k_2-k_5}\cdot\frac{\alpha_4 k_3}{k_3-k_5} \quad (2\ \overrightarrow{\alpha_2}\ 3\ \overrightarrow{\alpha_4}\ 5)\\
S^{-}_{6,2} &= \frac{\alpha_2 k_2}{k_2-k_6}\cdot\frac{\alpha_3 k_3}{k_3-k_6}\cdot\frac{\alpha_5 k_4}{k_4-k_6} \quad (2\ \overrightarrow{\alpha_2}\ 3\ \overrightarrow{\alpha_3}\ 4\ \overrightarrow{\alpha_5}\ 6)\\
&+ \frac{\alpha_2 k_2}{k_2-k_6}\cdot\frac{\alpha_3 k_3}{k_3-k_6}\cdot\frac{\alpha_6 k_4}{k_4-k_6}\cdot\frac{k_5}{k_5-k_6} \quad (2\ \overrightarrow{\alpha_2}\ 3\ \overrightarrow{\alpha_3}\ 4\ \overrightarrow{\alpha_6}\ 5\to 6)\\
&+ \frac{\alpha_2 k_2}{k_2-k_6}\cdot\frac{\alpha_4 k_3}{k_3-k_6}\cdot\frac{k_5}{k_5-k_6} \quad (2\ \overrightarrow{\alpha_2}\ 3\ \overrightarrow{\alpha_4}\ 5\to 6)\\
S^{-}_{7,2} &= \frac{\alpha_2 k_2}{k_2-k_7}\cdot\frac{\alpha_3 k_3}{k_3-k_7}\cdot\frac{\alpha_5 k_4}{k_4-k_7}\cdot\frac{\alpha_7 k_6}{k_6-k_7} \quad (2\ \overrightarrow{\alpha_2}\ 3\ \overrightarrow{\alpha_3}\ 4\ \overrightarrow{\alpha_5}\ 6\ \overrightarrow{\alpha_7}\ 7)\\
&+ \frac{\alpha_2 k_2}{k_2-k_7}\cdot\frac{\alpha_3 k_3}{k_3-k_7}\cdot\frac{\alpha_6 k_4}{k_4-k_7}\cdot\frac{k_5}{k_5-k_7}\cdot\frac{\alpha_7 k_6}{k_6-k_7} \quad (2\ \overrightarrow{\alpha_2}\ 3\ \overrightarrow{\alpha_3}\ 4\ \overrightarrow{\alpha_6}\ 5\to 6\ \overrightarrow{\alpha_7}\ 7)\\
&+ \frac{\alpha_2 k_2}{k_2-k_7}\cdot\frac{\alpha_4 k_3}{k_3-k_7}\cdot\frac{k_5}{k_5-k_7}\cdot\frac{\alpha_7 k_6}{k_6-k_7} \quad (2\ \overrightarrow{\alpha_2}\ 3\ \overrightarrow{\alpha_4}\ 5\to 6\ \overrightarrow{\alpha_7}\ 7)\\
S^{-}_{8,2} &= \frac{\alpha_2 k_2}{k_2-k_8}\cdot\frac{\alpha_3 k_3}{k_3-k_8}\cdot\frac{\alpha_5 k_4}{k_4-k_8}\cdot\frac{\alpha_7 k_6}{k_6-k_8}\cdot\frac{k_7}{k_7-k_8} \quad (2\ \overrightarrow{\alpha_2}\ 3\ \overrightarrow{\alpha_3}\ 4\ \overrightarrow{\alpha_5}\ 6\ \overrightarrow{\alpha_7}\ 7\to 8)\\
&+ \frac{\alpha_2 k_2}{k_2-k_8}\cdot\frac{\alpha_3 k_3}{k_3-k_8}\cdot\frac{\alpha_5 k_4}{k_4-k_8}\cdot\frac{\alpha_8 k_6}{k_6-k_8} \quad (2\ \overrightarrow{\alpha_2}\ 3\ \overrightarrow{\alpha_3}\ 4\ \overrightarrow{\alpha_5}\ 6\ \overrightarrow{\alpha_8}\ 8)\\
&+ \frac{\alpha_2 k_2}{k_2-k_8}\cdot\frac{\alpha_3 k_3}{k_3-k_8}\cdot\frac{\alpha_6 k_4}{k_4-k_8}\cdot\frac{k_5}{k_5-k_8}\cdot\frac{\alpha_7 k_6}{k_6-k_8}\cdot\frac{k_7}{k_7-k_8} \quad (2\ \overrightarrow{\alpha_2}\ 3\ \overrightarrow{\alpha_3}\ 4\ \overrightarrow{\alpha_6}\ 5\to 6\ \overrightarrow{\alpha_7}\ 7\to 8)\\
&+ \frac{\alpha_2 k_2}{k_2-k_8}\cdot\frac{\alpha_3 k_3}{k_3-k_8}\cdot\frac{\alpha_6 k_4}{k_4-k_8}\cdot\frac{k_5}{k_5-k_8}\cdot\frac{\alpha_8 k_6}{k_6-k_8} \quad (2\ \overrightarrow{\alpha_2}\ 3\ \overrightarrow{\alpha_3}\ 4\ \overrightarrow{\alpha_6}\ 5\to 6\ \overrightarrow{\alpha_8}\ 8)\\
&+ \frac{\alpha_2 k_2}{k_2-k_8}\cdot\frac{\alpha_4 k_3}{k_3-k_8}\cdot\frac{k_5}{k_5-k_8}\cdot\frac{\alpha_7 k_6}{k_6-k_8}\cdot\frac{k_7}{k_7-k_8} \quad (2\ \overrightarrow{\alpha_2}\ 3\ \overrightarrow{\alpha_4}\ 5\to 6\ \overrightarrow{\alpha_7}\ 7\to 8)\\
&+ \frac{\alpha_2 k_2}{k_2-k_8}\cdot\frac{\alpha_4 k_3}{k_3-k_8}\cdot\frac{k_5}{k_5-k_8}\cdot\frac{\alpha_8 k_6}{k_6-k_8} \quad (2\ \overrightarrow{\alpha_2}\ 3\ \overrightarrow{\alpha_4}\ 5\to 6\ \overrightarrow{\alpha_8}\ 8)\\
S^{-}_{5,3} &= \frac{\alpha_3 k_3}{k_3-k_5}\cdot\frac{\alpha_6 k_4}{k_4-k_5} \quad (3\ \overrightarrow{\alpha_3}\ 4\ \overrightarrow{\alpha_6}\ 5)\\
&+ \frac{\alpha_4 k_3}{k_3-k_5} \quad (3\ \overrightarrow{\alpha_4}\ 5)\\
S^{-}_{6,3} &= \frac{\alpha_3 k_3}{k_3-k_6}\cdot\frac{\alpha_5 k_4}{k_4-k_6} \quad (3\ \overrightarrow{\alpha_3}\ 4\ \overrightarrow{\alpha_5}\ 6)\\
&+ \frac{\alpha_3 k_3}{k_3-k_6}\cdot\frac{\alpha_6 k_4}{k_4-k_6}\cdot\frac{k_5}{k_5-k_6} \quad (3\ \overrightarrow{\alpha_3}\ 4\ \overrightarrow{\alpha_6}\ 5\to 6)\\
&+ \frac{\alpha_4 k_3}{k_3-k_6}\cdot\frac{k_5}{k_5-k_6} \quad (3\ \overrightarrow{\alpha_4}\ 5\to 6)\\
S^{-}_{7,3} &= \frac{\alpha_3 k_3}{k_3-k_7}\cdot\frac{\alpha_5 k_4}{k_4-k_7}\cdot\frac{\alpha_7 k_6}{k_6-k_7} \quad (3\ \overrightarrow{\alpha_3}\ 4\ \overrightarrow{\alpha_5}\ 6\ \overrightarrow{\alpha_7}\ 7)\\
&+ \frac{\alpha_3 k_3}{k_3-k_7}\cdot\frac{\alpha_6 k_4}{k_4-k_7}\cdot\frac{k_5}{k_5-k_7}\cdot\frac{\alpha_7 k_6}{k_6-k_7} \quad (3\ \overrightarrow{\alpha_3}\ 4\ \overrightarrow{\alpha_6}\ 5\ \to 6\ \overrightarrow{\alpha_7}\ 7)\\
&+ \frac{\alpha_4 k_3}{k_3-k_7}\cdot\frac{k_5}{k_5-k_7}\cdot\frac{\alpha_7 k_6}{k_6-k_7} \quad (3\ \overrightarrow{\alpha_4}\ 5\to 6\ \overrightarrow{\alpha_7}\ 7)\\
S^{-}_{8,3} &= \frac{\alpha_3 k_3}{k_3-k_8}\cdot\frac{\alpha_5 k_4}{k_4-k_8}\cdot\frac{\alpha_7 k_6}{k_6-k_8}\cdot\frac{k_7}{k_7-k_8} \quad (3\ \overrightarrow{\alpha_3}\ 4\ \overrightarrow{\alpha_5}\ 6\ \overrightarrow{\alpha_7}\ 7\to 8)
\end{aligned}
$$

$$
\begin{aligned}
&+ \quad \frac{\alpha_3 k_3}{k_3-k_8}\cdot\frac{\alpha_5 k_4}{k_4-k_8}\cdot\frac{\alpha_8 k_6}{k_6-k_8} \quad (3\ \overrightarrow{\alpha_3}\ 4\ \overrightarrow{\alpha_5}\ 6\ \overrightarrow{\alpha_8}\ 8)\\
&+ \quad \frac{\alpha_3 k_3}{k_3-k_8}\cdot\frac{\alpha_6 k_4}{k_4-k_8}\cdot\frac{k_5}{k_5-k_8}\cdot\frac{\alpha_7 k_6}{k_6-k_8}\cdot\frac{k_7}{k_7-k_8} \quad (3\ \overrightarrow{\alpha_3}\ 4\ \overrightarrow{\alpha_6}\ 5\to 6\ \overrightarrow{\alpha_7}\ 7\to 8)\\
&+ \quad \frac{\alpha_3 k_3}{k_3-k_8}\cdot\frac{\alpha_6 k_4}{k_4-k_8}\cdot\frac{k_5}{k_5-k_8}\cdot\frac{\alpha_8 k_6}{k_6-k_8} \quad (3\ \overrightarrow{\alpha_3}\ 4\ \overrightarrow{\alpha_6}\ 5\to 6\ \overrightarrow{\alpha_8}\ 8)\\
&+ \quad \frac{\alpha_4 k_3}{k_3-k_8}\cdot\frac{k_5}{k_5-k_8}\cdot\frac{\alpha_7 k_6}{k_6-k_8}\cdot\frac{k_7}{k_7-k_8} \quad (3\ \overrightarrow{\alpha_4}\ 5\to 6\ \overrightarrow{\alpha_7}\ 7\to 8)\\
&+ \quad \frac{\alpha_4 k_3}{k_3-k_8}\cdot\frac{k_5}{k_5-k_8}\cdot\frac{\alpha_8 k_6}{k_6-k_8} \quad (3\ \overrightarrow{\alpha_4}\ 5\to 6\ \overrightarrow{\alpha_8}\ 8)\\
S^-_{6,4} &= \quad \frac{\alpha_5 k_4}{k_4-k_6} \quad (4\ \overrightarrow{\alpha_5}\ 6)\\
&+ \quad \frac{\alpha_6 k_4}{k_4-k_6}\cdot\frac{k_5}{k_5-k_6} \quad (4\ \overrightarrow{\alpha_6}\ 5\to 6)\\
S^-_{7,4} &= \quad \frac{\alpha_5 k_4}{k_4-k_7}\cdot\frac{\alpha_7 k_6}{k_6-k_7} \quad (4\ \overrightarrow{\alpha_5}\ 6\ \overrightarrow{\alpha_7}\ 7)\\
&+ \quad \frac{\alpha_6 k_4}{k_4-k_7}\cdot\frac{k_5}{k_5-k_7}\cdot\frac{\alpha_7 k_6}{k_6-k_7} \quad (4\ \overrightarrow{\alpha_6}\ 5\to 6\ \overrightarrow{\alpha_7}\ 7)\\
S^-_{8,4} &= \quad \frac{\alpha_5 k_4}{k_4-k_8}\cdot\frac{\alpha_7 k_6}{k_6-k_8}\cdot\frac{k_7}{k_7-k_8} \quad (4\ \overrightarrow{\alpha_5}\ 6\ \overrightarrow{\alpha_7}\ 7\to 8)\\
&+ \quad \frac{\alpha_5 k_4}{k_4-k_8}\cdot\frac{\alpha_8 k_6}{k_6-k_8} \quad (4\ \overrightarrow{\alpha_5}\ 6\ \overrightarrow{\alpha_8}\ 8)\\
&+ \quad \frac{\alpha_6 k_4}{k_4-k_8}\cdot\frac{k_5}{k_5-k_8}\cdot\frac{\alpha_7 k_6}{k_6-k_8}\cdot\frac{k_7}{k_7-k_8} \quad (4\ \overrightarrow{\alpha_6}\ 5\ \to 6\ \overrightarrow{\alpha_7}\ 7\to 8)\\
&+ \quad \frac{\alpha_6 k_4}{k_4-k_8}\cdot\frac{k_5}{k_5-k_8}\cdot\frac{\alpha_8 k_6}{k_6-k_8} \quad (4\ \overrightarrow{\alpha_6}\ 5\ \to 6\ \overrightarrow{\alpha_8}\ 8)\\
S^-_{7,5} &= \quad \frac{k_5}{k_5-k_7}\cdot\frac{\alpha_7 k_6}{k_6-k_7} \quad (5\to 6\ \overrightarrow{\alpha_7}\ 7)\\
S^-_{8,5} &= \quad \frac{k_5}{k_5-k_8}\cdot\frac{\alpha_7 k_6}{k_6-k_8}\cdot\frac{k_7}{k_7-k_8} \quad (5\to 6\ \overrightarrow{\alpha_7}\ 7\to 8)\\
&+ \quad \frac{k_5}{k_5-k_8}\cdot\frac{\alpha_8 k_6}{k_6-k_8} \quad (5\to 6\ \overrightarrow{\alpha_8}\ 8)\\
S^-_{8,6} &= \quad \frac{\alpha_7 k_6}{k_6-k_8}\cdot\frac{k_7}{k_7-k_8} \quad (6\ \overrightarrow{\alpha_7}\ 7\to 8)\\
&+ \quad \frac{\alpha_8 k_6}{k_6-k_8} \quad (6\ \overrightarrow{\alpha_8}\ 8),
\end{aligned}
$$

and

$$
\mathbf{S} = \begin{bmatrix}
1 & 0 & 0 & 0 & 0 & 0 & 0 & 0\\
\frac{\alpha_1 k_1}{k_2-k_1} & 1 & 0 & 0 & 0 & 0 & 0 & 0\\
S_{3,1} & \frac{\alpha_2 k_2}{k_3-k_2} & 1 & 0 & 0 & 0 & 0 & 0\\
S_{4,1} & S_{4,2} & \frac{\alpha_3 k_3}{k_4-k_3} & 1 & 0 & 0 & 0 & 0\\
S_{5,1} & S_{5,2} & S_{5,3} & \frac{\alpha_6 k_4}{k_5-k_4} & 1 & 0 & 0 & 0\\
S_{6,1} & S_{6,2} & S_{6,3} & S_{6,4} & \frac{k_5}{k_6-k_5} & 1 & 0 & 0\\
S_{7,1} & S_{7,2} & S_{7,3} & S_{7,4} & S_{7,5} & \frac{\alpha_7 k_6}{k_7-k_6} & 1 & 0\\
S_{8,1} & S_{8,2} & S_{8,3} & S_{8,4} & S_{8,5} & S_{8,6} & \frac{k_7}{k_8-k_7} & 1
\end{bmatrix} \tag{11}
$$

where

$$
\begin{aligned}
S_{3,1} &= \frac{\alpha_1 k_1}{k_3-k_1}\cdot\frac{\alpha_2 k_2}{k_2-k_1} \quad (1\ \overrightarrow{\alpha_1}\ 2\ \overrightarrow{\alpha_2}\ 3)\\
S_{4,1} &= \frac{\alpha_1 k_1}{k_4-k_1}\cdot\frac{\alpha_2 k_2}{k_2-k_1}\cdot\frac{\alpha_3 k_3}{k_3-k_1} \quad (1\ \overrightarrow{\alpha_1}\ 2\ \overrightarrow{\alpha_2}\ 3\ \overrightarrow{\alpha_3}\ 4)\\
S_{5,1} &= \frac{\alpha_1 k_1}{k_5-k_1}\cdot\frac{\alpha_2 k_2}{k_2-k_1}\cdot\frac{\alpha_3 k_3}{k_3-k_1}\cdot\frac{\alpha_6 k_4}{k_4-k_1} \quad (1\ \overrightarrow{\alpha_1}\ 2\ \overrightarrow{\alpha_2}\ 3\ \overrightarrow{\alpha_3}\ 4\ \overrightarrow{\alpha_6}\ 5)\\
&+ \frac{\alpha_1 k_1}{k_5-k_1}\cdot\frac{\alpha_2 k_2}{k_2-k_1}\cdot\frac{\alpha_4 k_3}{k_3-k_1} \quad (1\ \overrightarrow{\alpha_1}\ 2\ \overrightarrow{\alpha_2}\ 3\ \overrightarrow{\alpha_4}\ 4)\\
S_{6,1} &= \frac{\alpha_1 k_1}{k_6-k_1}\cdot\frac{\alpha_2 k_2}{k_2-k_1}\cdot\frac{\alpha_3 k_3}{k_3-k_1}\cdot\frac{\alpha_6 k_4}{k_4-k_1}\cdot\frac{k_5}{k_5-k_1} \quad (1\ \overrightarrow{\alpha_1}\ 2\ \overrightarrow{\alpha_2}\ 3\ \overrightarrow{\alpha_3}\ 4\ \overrightarrow{\alpha_6}\ 5\to 6)\\
&+ \frac{\alpha_1 k_1}{k_6-k_1}\cdot\frac{\alpha_2 k_2}{k_2-k_1}\cdot\frac{\alpha_3 k_3}{k_3-k_1}\cdot\frac{\alpha_5 k_4}{k_4-k_1} \quad (1\ \overrightarrow{\alpha_1}\ 2\ \overrightarrow{\alpha_2}\ 3\ \overrightarrow{\alpha_3}\ 4\ \overrightarrow{\alpha_5}\ 6)\\
&+ \frac{\alpha_1 k_1}{k_6-k_1}\cdot\frac{\alpha_2 k_2}{k_2-k_1}\cdot\frac{\alpha_4 k_3}{k_3-k_1}\cdot\frac{k_5}{k_5-k_1} \quad (1\ \overrightarrow{\alpha_1}\ 2\ \overrightarrow{\alpha_2}\ 3\ \overrightarrow{\alpha_4}\ 5\to 6)\\
S_{7,1} &= \frac{\alpha_1 k_1}{k_7-k_1}\cdot\frac{\alpha_2 k_2}{k_2-k_1}\cdot\frac{\alpha_3 k_3}{k_3-k_1}\cdot\frac{\alpha_5 k_4}{k_4-k_1}\cdot\frac{\alpha_7 k_6}{k_6-k_1} \quad (1\ \overrightarrow{\alpha_1}\ 2\ \overrightarrow{\alpha_2}\ 3\ \overrightarrow{\alpha_5}\ 6\ \overrightarrow{\alpha_7}\ 7)\\
&+ \frac{\alpha_1 k_1}{k_7-k_1}\cdot\frac{\alpha_2 k_2}{k_2-k_1}\cdot\frac{\alpha_3 k_3}{k_3-k_1}\cdot\frac{\alpha_6 k_4}{k_4-k_1}\cdot\frac{k_5}{k_5-k_1}\cdot\frac{\alpha_7 k_6}{k_6-k_1} \quad (1\ \overrightarrow{\alpha_1}\ 2\ \overrightarrow{\alpha_2}\ 3\ \overrightarrow{\alpha_3}\ 4\ \overrightarrow{\alpha_6}\ 5\to 6\ \overrightarrow{\alpha_7}\ 7)\\
&+ \frac{\alpha_1 k_1}{k_7-k_1}\cdot\frac{\alpha_2 k_2}{k_2-k_1}\cdot\frac{\alpha_4 k_3}{k_3-k_1}\cdot\frac{k_5}{k_5-k_1}\cdot\frac{\alpha_7 k_6}{k_6-k_1} \quad (1\ \overrightarrow{\alpha_1}\ 2\ \overrightarrow{\alpha_2}\ 3\ \overrightarrow{\alpha_4}\ 5\to 6\ \overrightarrow{\alpha_7}\ 7)\\
S_{8,1} &= \frac{\alpha_1 k_1}{k_8-k_1}\cdot\frac{\alpha_2 k_2}{k_2-k_1}\cdot\frac{\alpha_3 k_3}{k_3-k_1}\cdot\frac{\alpha_5 k_4}{k_4-k_1}\cdot\frac{\alpha_7 k_6}{k_6-k_1}\cdot\frac{k_7}{k_7-k_1} \quad (1\ \overrightarrow{\alpha_1}\ 2\ \overrightarrow{\alpha_2}\ 3\ \overrightarrow{\alpha_3}\ 4\ \overrightarrow{\alpha_5}\ 6\ \overrightarrow{\alpha_7}\ 7\to 8)\\
&+ \frac{\alpha_1 k_1}{k_8-k_1}\cdot\frac{\alpha_2 k_2}{k_2-k_1}\cdot\frac{\alpha_3 k_3}{k_3-k_1}\cdot\frac{\alpha_5 k_4}{k_4-k_1}\cdot\frac{\alpha_8 k_6}{k_6-k_1} \quad (1\ \overrightarrow{\alpha_1}\ 2\ \overrightarrow{\alpha_2}\ 3\ \overrightarrow{\alpha_3}\ 4\ \overrightarrow{\alpha_5}\ 6\ \overrightarrow{\alpha_8}\ 8)\\
&+ \frac{\alpha_1 k_1}{k_8-k_1}\cdot\frac{\alpha_2 k_2}{k_2-k_1}\cdot\frac{\alpha_3 k_3}{k_3-k_1}\cdot\frac{\alpha_6 k_4}{k_4-k_1}\cdot\frac{k_5}{k_5-k_1}\cdot\frac{\alpha_7 k_6}{k_6-k_1}\cdot\frac{k_7}{k_7-k_1} \quad (1\ \overrightarrow{\alpha_1}\ 2\ \overrightarrow{\alpha_2}\ 3\ \overrightarrow{\alpha_3}\ 4\ \overrightarrow{\alpha_6}\ 5\ \to 6\ \overrightarrow{\alpha_7}\ 7\to 8)\\
&+ \frac{\alpha_1 k_1}{k_8-k_1}\cdot\frac{\alpha_2 k_2}{k_2-k_1}\cdot\frac{\alpha_3 k_3}{k_3-k_1}\cdot\frac{\alpha_6 k_4}{k_4-k_1}\cdot\frac{k_5}{k_5-k_1}\cdot\frac{\alpha_8 k_6}{k_6-k_1} \quad (1\ \overrightarrow{\alpha_1}\ 2\ \overrightarrow{\alpha_3}\ 3\ \overrightarrow{\alpha_3}\ 4\ \overrightarrow{\alpha_6}\ 5\to 6\ \overrightarrow{\alpha_8}\ 8)\\
&+ \frac{\alpha_1 k_1}{k_8-k_1}\cdot\frac{\alpha_2 k_2}{k_2-k_1}\cdot\frac{\alpha_4 k_3}{k_3-k_1}\cdot\frac{k_5}{k_5-k_1}\cdot\frac{\alpha_7 k_6}{k_6-k_1}\cdot\frac{k_7}{k_7-k_1} \quad (1\ \overrightarrow{\alpha_1}\ 2\ \overrightarrow{\alpha_2}\ 3\ \overrightarrow{\alpha_4}\ 5\to 6\ \overrightarrow{\alpha_7}\ 7\to 8)\\
&+ \frac{\alpha_1 k_1}{k_8-k_1}\cdot\frac{\alpha_2 k_2}{k_2-k_1}\cdot\frac{\alpha_4 k_3}{k_3-k_1}\cdot\frac{k_5}{k_5-k_1}\cdot\frac{\alpha_8 k_6}{k_6-k_1} \quad (1\ \overrightarrow{\alpha_1}\ 2\ \overrightarrow{\alpha_2}\ 3\ \overrightarrow{\alpha_4}\ 5\to 6\ \overrightarrow{\alpha_8}\ 8)\\
S_{4,2} &= \frac{\alpha_2 k_2}{k_4-k_2}\cdot\frac{\alpha_3 k_3}{k_3-k_2} \quad (2\ \overrightarrow{\alpha_2}\ 3\ \overrightarrow{\alpha_3}\ 4)\\
S_{5,2} &= \frac{\alpha_2 k_2}{k_5-k_2}\cdot\frac{\alpha_3 k_3}{k_3-k_2}\cdot\frac{\alpha_6 k_4}{k_4-k_2} \quad (2\ \overrightarrow{\alpha_2}\ 3\ \overrightarrow{\alpha_3}\ 4\ \overrightarrow{\alpha_6}\ 5)\\
&+ \frac{\alpha_2 k_2}{k_5-k_2}\cdot\frac{\alpha_4 k_3}{k_3-k_2} \quad (2\ \overrightarrow{\alpha_2}\ 3\ \overrightarrow{\alpha_4}\ 5)\\
S_{6,2} &= \frac{\alpha_2 k_2}{k_6-k_2}\cdot\frac{\alpha_3 k_3}{k_3-k_2}\cdot\frac{\alpha_5 k_4}{k_4-k_2} \quad (2\ \overrightarrow{\alpha_2}\ 3\ \overrightarrow{\alpha_3}\ 4\ \overrightarrow{\alpha_5}\ 6)\\
&+ \frac{\alpha_2 k_2}{k_6-k_2}\cdot\frac{\alpha_3 k_3}{k_3-k_2}\cdot\frac{\alpha_6 k_4}{k_4-k_2}\cdot\frac{k_5}{k_5-k_2} \quad (2\ \overrightarrow{\alpha_2}\ 3\ \overrightarrow{\alpha_3}\ 4\ \overrightarrow{\alpha_6}\ 5\to 6)\\
&+ \frac{\alpha_2 k_2}{k_6-k_2}\cdot\frac{\alpha_4 k_3}{k_3-k_2}\cdot\frac{k_5}{k_5-k_2} \quad (2\ \overrightarrow{\alpha_2}\ 3\ \overrightarrow{\alpha_4}\ 5\to 6)\\
S_{7,2} &= \frac{\alpha_2 k_2}{k_7-k_2}\cdot\frac{\alpha_3 k_3}{k_3-k_2}\cdot\frac{\alpha_5 k_4}{k_4-k_2}\cdot\frac{\alpha_7 k_6}{k_6-k_2} \quad (2\ \overrightarrow{\alpha_2}\ 3\ \overrightarrow{\alpha_3}\ 4\ \overrightarrow{\alpha_5}\ 6\ \overrightarrow{\alpha_7}\ 7)
\end{aligned}
$$

$$
\begin{aligned}
&+ \quad \frac{\alpha_2 k_2}{k_7-k_2}\cdot\frac{\alpha_3 k_3}{k_3-k_2}\cdot\frac{\alpha_6 k_4}{k_4-k_2}\cdot\frac{k_5}{k_5-k_2}\cdot\frac{\alpha_7 k_6}{k_6-k_2} \quad (2\ \overrightarrow{\alpha_2}\ 3\ \overrightarrow{\alpha_3}\ 4\ \overrightarrow{\alpha_6}\ 5\to 6\ \overrightarrow{\alpha_7}\ 7)\\
&+ \quad \frac{\alpha_2 k_2}{k_7-k_2}\cdot\frac{\alpha_4 k_3}{k_3-k_2}\cdot\frac{k_5}{k_5-k_2}\cdot\frac{\alpha_7 k_6}{k_6-k_2} \quad (2\ \overrightarrow{\alpha_2}\ 3\ \overrightarrow{\alpha_4}\ 5\to 6\ \overrightarrow{\alpha_7}\ 7)\\
S_{8,2} \;&= \quad \frac{\alpha_2 k_2}{k_8-k_2}\cdot\frac{\alpha_3 k_3}{k_3-k_2}\cdot\frac{\alpha_5 k_4}{k_4-k_2}\cdot\frac{\alpha_7 k_6}{k_6-k_2}\cdot\frac{k_7}{k_7-k_2} \quad (2\ \overrightarrow{\alpha_2}\ 3\ \overrightarrow{\alpha_3}\ 4\ \overrightarrow{\alpha_5}\ 6\ \overrightarrow{\alpha_7}\ 7\to 8)\\
&+ \quad \frac{\alpha_2 k_2}{k_8-k_2}\cdot\frac{\alpha_3 k_3}{k_3-k_2}\cdot\frac{\alpha_5 k_4}{k_4-k_2}\cdot\frac{\alpha_8 k_6}{k_6-k_2} \quad (2\ \overrightarrow{\alpha_2}\ 3\ \overrightarrow{\alpha_3}\ 4\ \overrightarrow{\alpha_5}\ 6\ \overrightarrow{\alpha_8}\ 8)\\
&+ \quad \frac{\alpha_2 k_2}{k_8-k_2}\cdot\frac{\alpha_3 k_3}{k_3-k_2}\cdot\frac{\alpha_6 k_4}{k_4-k_2}\cdot\frac{k_5}{k_5-k_2}\cdot\frac{\alpha_7 k_6}{k_6-k_2}\cdot\frac{k_7}{k_7-k_2} \quad (2\ \overrightarrow{\alpha_2}\ 3\ \overrightarrow{\alpha_3}\ 4\ \overrightarrow{\alpha_6}\ 5\to 6\ \overrightarrow{\alpha_7}\ 7\to 8)\\
&+ \quad \frac{\alpha_2 k_2}{k_8-k_2}\cdot\frac{\alpha_3 k_3}{k_3-k_2}\cdot\frac{\alpha_6 k_4}{k_4-k_2}\cdot\frac{k_5}{k_5-k_2}\cdot\frac{\alpha_8 k_6}{k_6-k_2} \quad (2\ \overrightarrow{\alpha_2}\ 3\ \overrightarrow{\alpha_3}\ 4\ \overrightarrow{\alpha_6}\ 5\to 6\ \overrightarrow{\alpha_8}\ 7)\\
&+ \quad \frac{\alpha_2 k_2}{k_8-k_2}\cdot\frac{\alpha_4 k_3}{k_3-k_2}\cdot\frac{k_5}{k_5-k_2}\cdot\frac{\alpha_7 k_6}{k_6-k_2}\cdot\frac{k_7}{k_7-k_2} \quad (2\ \overrightarrow{\alpha_2}\ 3\ \overrightarrow{\alpha_4}\ 5\to 6\ \overrightarrow{\alpha_7}\ 7\to 8)\\
&+ \quad \frac{\alpha_2 k_2}{k_8-k_2}\cdot\frac{\alpha_4 k_3}{k_3-k_2}\cdot\frac{k_5}{k_5-k_2}\cdot\frac{\alpha_8 k_6}{k_6-k_2} \quad (2\ \overrightarrow{\alpha_2}\ 3\ \overrightarrow{\alpha_4}\ 5\to 6\ \overrightarrow{\alpha_8}\ 8)\\
S_{5,3} \;&= \quad \frac{\alpha_3 k_3}{k_5-k_3}\cdot\frac{\alpha_6 k_4}{k_4-k_3} \quad (3\ \overrightarrow{\alpha_3}\ 4\ \overrightarrow{\alpha_6}\ 5)\\
&+ \quad \frac{\alpha_4 k_3}{k_5-k_3} \quad (3\ \overrightarrow{\alpha_4}\ 5)\\
S_{6,3} \;&= \quad \frac{\alpha_3 k_3}{k_6-k_3}\cdot\frac{\alpha_5 k_4}{k_4-k_3} \quad (3\ \overrightarrow{\alpha_3}\ 4\ \overrightarrow{\alpha_5}\ 6)\\
&+ \quad \frac{\alpha_3 k_3}{k_6-k_3}\cdot\frac{\alpha_6 k_4}{k_4-k_3}\cdot\frac{k_5}{k_5-k_3} \quad (3\ \overrightarrow{\alpha_3}\ 4\ \overrightarrow{\alpha_6}\ 5\to 6)\\
&+ \quad \frac{\alpha_4 k_3}{k_6-k_3}\cdot\frac{k_5}{k_5-k_3} \quad (3\ \overrightarrow{\alpha_4}\ 5\to 6)\\
S_{7,3} \;&= \quad \frac{\alpha_3 k_3}{k_7-k_3}\cdot\frac{\alpha_5 k_4}{k_4-k_3}\cdot\frac{\alpha_7 k_6}{k_6-k_3} \quad (3\ \overrightarrow{\alpha_3}\ 4\ \overrightarrow{\alpha_5}\ 6\ \overrightarrow{\alpha_7}\ 7)\\
&+ \quad \frac{\alpha_3 k_3}{k_7-k_3}\cdot\frac{\alpha_6 k_4}{k_4-k_3}\cdot\frac{k_5}{k_5-k_3}\cdot\frac{\alpha_7 k_6}{k_6-k_3} \quad (3\ \overrightarrow{\alpha_3}\ 4\ \overrightarrow{\alpha_6}\ 5\ \to 6\ \overrightarrow{\alpha_7}\ 7)\\
&+ \quad \frac{\alpha_4 k_3}{k_7-k_3}\cdot\frac{k_5}{k_5-k_3}\cdot\frac{\alpha_7 k_6}{k_6-k_3} \quad (3\ \overrightarrow{\alpha_4}\ 5\to 6\ \overrightarrow{\alpha_7}\ 7)\\
S_{8,3} \;&= \quad \frac{\alpha_3 k_3}{k_8-k_3}\cdot\frac{\alpha_5 k_4}{k_4-k_3}\cdot\frac{\alpha_7 k_6}{k_6-k_3}\cdot\frac{k_7}{k_7-k_3} \quad (3\ \overrightarrow{\alpha_3}\ 4\ \overrightarrow{\alpha_5}\ 6\ \overrightarrow{\alpha_7}\ 7\to 8)\\
&+ \quad \frac{\alpha_3 k_3}{k_8-k_3}\cdot\frac{\alpha_5 k_4}{k_4-k_3}\cdot\frac{\alpha_8 k_6}{k_6-k_3} \quad (3\ \overrightarrow{\alpha_3}\ 4\ \overrightarrow{\alpha_5}\ 6\ \overrightarrow{\alpha_8}\ 8)\\
&+ \quad \frac{\alpha_3 k_3}{k_8-k_3}\cdot\frac{\alpha_6 k_4}{k_4-k_3}\cdot\frac{k_5}{k_5-k_3}\cdot\frac{\alpha_7 k_6}{k_6-k_3}\cdot\frac{k_7}{k_7-k_3} \quad (3\ \overrightarrow{\alpha_3}\ 4\ \overrightarrow{\alpha_6}\ 5\to 6\ \overrightarrow{\alpha_7}\ 7\to 8)\\
&+ \quad \frac{\alpha_3 k_3}{k_8-k_3}\cdot\frac{\alpha_6 k_4}{k_4-k_3}\cdot\frac{k_5}{k_5-k_3}\cdot\frac{\alpha_8 k_6}{k_6-k_3} \quad (3\ \overrightarrow{\alpha_3}\ 4\ \overrightarrow{\alpha_6}\ 5\to 6\ \overrightarrow{\alpha_8}\ 8)\\
&+ \quad \frac{\alpha_4 k_3}{k_8-k_3}\cdot\frac{k_5}{k_5-k_3}\cdot\frac{\alpha_7 k_6}{k_6-k_3}\cdot\frac{k_7}{k_7-k_3} \quad (3\ \overrightarrow{\alpha_4}\ 5\to 6\ \overrightarrow{\alpha_7}\ 7\to 8)\\
&+ \quad \frac{\alpha_4 k_3}{k_8-k_3}\cdot\frac{k_5}{k_5-k_3}\cdot\frac{\alpha_8 k_6}{k_6-k_3} \quad (3\ \overrightarrow{\alpha_4}\ 5\to 6\ \overrightarrow{\alpha_8}\ 8)\\
S_{6,4} \;&= \quad \frac{\alpha_5 k_4}{k_6-k_4} \quad (4\ \overrightarrow{\alpha_5}\ 6)\\
&+ \quad \frac{\alpha_6 k_4}{k_6-k_4}\cdot\frac{k_5}{k_5-k_4} \quad (4\ \overrightarrow{\alpha_6}\ 5\to 6)
\end{aligned}
$$

$$
\begin{aligned}
S_{7,4} &= \frac{\alpha_5 k_4}{k_7-k_4}\cdot\frac{\alpha_7 k_6}{k_6-k_4} \quad (4\ \overrightarrow{\alpha_5}\ 6\ \overrightarrow{\alpha_7}\ 7)\\
&+ \frac{\alpha_6 k_4}{k_7-k_4}\cdot\frac{k_5}{k_5-k_4}\cdot\frac{\alpha_7 k_6}{k_6-k_4} \quad (4\ \overrightarrow{\alpha_6}\ 5\rightarrow 6\ \overrightarrow{\alpha_7}\ 7)\\
S_{8,4} &= \frac{\alpha_5 k_4}{k_8-k_4}\cdot\frac{\alpha_7 k_6}{k_6-k_4}\cdot\frac{k_7}{k_7-k_4} \quad (4\ \overrightarrow{\alpha_5}\ 6\ \overrightarrow{\alpha_7}\ 7\rightarrow 8)\\
&+ \frac{\alpha_5 k_4}{k_8-k_4}\cdot\frac{\alpha_8 k_6}{k_6-k_4} \quad (4\ \overrightarrow{\alpha_5}\ 6\ \overrightarrow{\alpha_8}\ 8)\\
&+ \frac{\alpha_6 k_4}{k_8-k_4}\cdot\frac{k_5}{k_5-k_4}\cdot\frac{\alpha_7 k_6}{k_6-k_4}\cdot\frac{k_7}{k_7-k_4} \quad (4\ \overrightarrow{\alpha_6}\ 5\ \rightarrow 6\ \overrightarrow{\alpha_7}\ 7\rightarrow 8)\\
&+ \frac{\alpha_6 k_4}{k_8-k_4}\cdot\frac{k_5}{k_5-k_4}\cdot\frac{\alpha_8 k_6}{k_6-k_4} \quad (4\ \overrightarrow{\alpha_6}\ 5\ \rightarrow 6\ \overrightarrow{\alpha_8}\ 8)\\
S_{7,5} &= \frac{k_5}{k_7-k_5}\cdot\frac{\alpha_7 k_6}{k_6-k_5} \quad (5\rightarrow 6\ \overrightarrow{\alpha_7}\ 7)\\
S_{8,5} &= \frac{k_5}{k_8-k_5}\cdot\frac{\alpha_7 k_6}{k_6-k_5}\cdot\frac{k_7}{k_7-k_5} \quad (5\rightarrow 6\ \overrightarrow{\alpha_7}\ 7\rightarrow 8)\\
&+ \frac{k_5}{k_8-k_5}\cdot\frac{\alpha_8 k_6}{k_6-k_5} \quad (5\rightarrow 6\ \overrightarrow{\alpha_8}\ 8)\\
S_{8,6} &= \frac{\alpha_7 k_6}{k_8-k_6}\cdot\frac{k_7}{k_7-k_6} \quad (6\ \overrightarrow{\alpha_7}\ 7\rightarrow 8)\\
&+ \frac{\alpha_8 k_6}{k_8-k_6} \quad (6\ \overrightarrow{\alpha_8}\ 8).
\end{aligned}
$$

Appendix B: Transformation Matrices of 135 Decay Network

Transformation matrices $\mathbf{S}^-$ and $\mathbf{S}$ of 135 decay networks are formulated as:

$$
\mathbf{S}^- = \begin{bmatrix}
1 & 0 & 0 & 0 & 0 & 0\\
\frac{k_1}{k_1-k_2} & 1 & 0 & 0 & 0 & 0\\
S^-_{3,1} & \frac{\alpha_1 k_2}{k_2-k_3} & 1 & 0 & 0 & 0\\
S^-_{4,1} & S^-_{4,2} & \frac{k_3}{k_3-k_4} & 1 & 0 & 0\\
S^-_{5,1} & S^-_{5,2} & S^-_{5,3} & \frac{\alpha_2 k_4}{k_4-k_5} & 1 & 0\\
S^-_{6,1} & S^-_{6,2} & S^-_{6,3} & S^-_{6,4} & \frac{k_5}{k_5-k_6} & 1
\end{bmatrix} \tag{12}
$$

where

$$
\begin{aligned}
S^-_{3,1} &= \frac{k_1}{k_1-k_3}\cdot\frac{\alpha_1 k_2}{k_2-k_3} \quad (1\rightarrow 2\ \overrightarrow{\alpha_1}\ 3)\\
S^-_{4,1} &= \frac{k_1}{k_1-k_4}\cdot\frac{\alpha_1 k_2}{k_2-k_4}\cdot\frac{k_3}{k_3-k_4} \quad (1\rightarrow 2\ \overrightarrow{\alpha_1}\ 2\rightarrow 3\rightarrow 4)\\
S^-_{5,1} &= \frac{k_1}{k_1-k_5}\cdot\frac{\alpha_1 k_2}{k_2-k_5}\cdot\frac{k_3}{k_3-k_5}\cdot\frac{\alpha_2 k_4}{k_4-k_5} \quad (1\rightarrow 2\ \overrightarrow{\alpha_1}\ 2\rightarrow 3\rightarrow 4\ \overrightarrow{\alpha_2}\ 5)\\
S^-_{6,1} &= \frac{k_1}{k_1-k_6}\cdot\frac{k_2}{k_2-k_6}\cdot\frac{\alpha_1\cdot k_3}{k_3-k_6}\cdot\frac{\alpha_3 k_4}{k_4-k_6} \quad (1\rightarrow 2\ \overrightarrow{\alpha_1}\ 2\rightarrow 3\rightarrow 4\ \overrightarrow{\alpha_3}\ 6)\\
&+ \frac{k1}{k_1-k_6}\cdot\frac{k_2}{k_2-k_6}\cdot\frac{\alpha_1 k_3}{k_3-k_6}\cdot\frac{\alpha_2 k_4}{k_4-k_6}\cdot\frac{k_5}{k_5-k_6} \quad (1\rightarrow 2\ \overrightarrow{\alpha_1}\ 2\rightarrow 3\rightarrow 4\ \overrightarrow{\alpha_2}\ 5\rightarrow 6)\\
S^-_{4,2} &= \frac{\alpha_1 k_2}{k_2-k_4}\cdot\frac{k_3}{k_3-k_4} \quad (2\ \overrightarrow{\alpha_1}\ 3\rightarrow 4)\\
S^-_{5,2} &= \frac{\alpha_1 k_2}{k_2-k_5}\cdot\frac{k_3}{k_k 3-k_5}\cdot\frac{\alpha_2 k_4}{k_4-k_5} \quad (2\ \overrightarrow{\alpha_1}\ 3\ \rightarrow 4\ \overrightarrow{\alpha_2}\ 5)
\end{aligned}
$$

$$
\begin{aligned}
S^-_{6,2} &= \frac{k_2}{k_2-k_6}\cdot\frac{\alpha_1\cdot k_3}{k_3-k_6}\cdot\frac{\alpha_3 k_4}{k_4-k_6} \quad (2\ \overrightarrow{\alpha_1}\ 2\to 3\to 4\ \overrightarrow{\alpha_3}\ 6)\\
&+ \cdot\frac{k_2}{k_2-k_6}\cdot\frac{\alpha_1 k_3}{k_3-k_6}\cdot\frac{\alpha_2 k_4}{k_4-k_6}\cdot\frac{k_5}{k_5-k_6} \quad (2\ \overrightarrow{\alpha_1}\ 3\to 4\ \overrightarrow{\alpha_2}\ 5\to 6)\\
S^-_{5,3} &= \frac{k_3}{k_3-k_5}\cdot\frac{\alpha_2 k_4}{k_4-k_5} \quad (3\to 4\ \overrightarrow{\alpha_2}\ 5)\\
S^-_{6,3} &= \frac{\alpha_1\cdot k_3}{k_3-k_6}\cdot\frac{\alpha_3 k_4}{k_4-k_6} \quad (3\to 4\ \overrightarrow{\alpha_3}\ 6)\\
&+ \frac{\alpha_1 k_3}{k_3-k_6}\cdot\frac{\alpha_2 k_4}{k_4-k_6}\cdot\frac{k_5}{k_5-k_6} \quad (3\to 4\ \overrightarrow{\alpha_2}\ 5\to 6)\\
S^-_{6,4} &= \frac{\alpha_3 k_4}{k_4-k_6} \quad (4\ \overrightarrow{\alpha_3}\ 6)\\
&+ \frac{\alpha_2 k_4}{k_4-k_6}\cdot\frac{k_5}{k_5-k_6} \quad (4\ \overrightarrow{\alpha_2}\ 5\to 6)
\end{aligned}
$$

and

$$
\mathbf{S}^- = \begin{bmatrix}
1 & 0 & 0 & 0 & 0 & 0\\
\frac{k_1}{k_2-k_1} & 1 & 0 & 0 & 0 & 0\\
S_{3,1} & \frac{\alpha_1 k_2}{k_3-k_2} & 1 & 0 & 0 & 0\\
S_{4,1} & S_{4,2} & \frac{k_3}{k_4-k_3} & 1 & 0 & 0\\
S_{5,1} & S_{5,2} & S_{5,3} & \frac{\alpha_2 k_4}{k_5-k_4} & 1 & 0\\
S_{6,1} & S_{6,2} & S_{6,3} & S_{6,4} & \frac{k_5}{k_6-k_3} & 1
\end{bmatrix} \tag{13}
$$

where

$$
\begin{aligned}
S_{3,1} &= \frac{k_1}{k_3-k_1}\cdot\frac{\alpha_1 k_2}{k_2-k_1} \quad (1\to 2\ \overrightarrow{\alpha_1}\ 3)\\
S_{4,1} &= \frac{k_1}{k_4-k_1}\cdot\frac{\alpha_1 k_2}{k_2-k_1}\cdot\frac{k_3}{k_3-k_1} \quad (1\to 2\ \overrightarrow{\alpha_1}\ 2\to 3\to 4)\\
S_{5,1} &= \frac{k_1}{k_5-k_1}\cdot\frac{\alpha_1 k_2}{k_2-k_1}\cdot\frac{k_3}{k_3-k_1}\cdot\frac{\alpha_2 k_4}{k_4-k_1} \quad (1\to 2\ \overrightarrow{\alpha_1}\ 2\to 3\to 4\ \overrightarrow{\alpha_2}\ 5)\\
S_{6,1} &= \frac{k_1}{k_6-k_1}\cdot\frac{k_2}{k_2-k_1}\cdot\frac{\alpha_1\cdot k_3}{k_3-k_1}\cdot\frac{\alpha_3 k_4}{k_4-k_1} \quad (1\to 2\ \overrightarrow{\alpha_1}\ 2\to 3\to 4\ \overrightarrow{\alpha_3}\ 6)\\
&+ \frac{k1}{k_6-k_1}\cdot\frac{k_2}{k_2-k_1}\cdot\frac{\alpha_1 k_3}{k_3-k_1}\cdot\frac{\alpha_2 k_4}{k_4-k_1}\cdot\frac{k_5}{k_5-k_1} \quad (1\to 2\ \overrightarrow{\alpha_1}\ 2\to 3\to 4\ \overrightarrow{\alpha_2}\ 5\to 6)\\
S_{4,2} &= \frac{\alpha_1 k_2}{k_4-k_2}\cdot\frac{k_3}{k_3-k_2} \quad (2\ \overrightarrow{\alpha_1}\ 3\to 4)\\
S_{5,2} &= \frac{\alpha_1 k_2}{k_5-k_2}\cdot\frac{k_3}{k_k 3-k_2}\cdot\frac{\alpha_2 k_4}{k_4-k_2} \quad (2\ \overrightarrow{\alpha_1}\ 3\ \to 4\ \overrightarrow{\alpha_2}\ 5)\\
S_{6,2} &= \frac{k_2}{k_6-k_2}\cdot\frac{\alpha_1\cdot k_3}{k_3-k_2}\cdot\frac{\alpha_3 k_4}{k_4-k_2} \quad (2\ \overrightarrow{\alpha_1}\ 2\to 3\to 4\ \overrightarrow{\alpha_3}\ 6)\\
&+ \cdot\frac{k_2}{k_2-k_6}\cdot\frac{\alpha_1 k_3}{k_3-k_6}\cdot\frac{\alpha_2 k_4}{k_4-k_6}\cdot\frac{k_5}{k_5-k_6} \quad (2\ \overrightarrow{\alpha_1}\ 3\to 4\ \overrightarrow{\alpha_2}\ 5\to 6)\\
S_{5,3} &= \frac{k_3}{k_5-k_3}\cdot\frac{\alpha_2 k_4}{k_4-k_3} \quad (3\to 4\ \overrightarrow{\alpha_2}\ 5)\\
S_{6,3} &= \frac{\alpha_1\cdot k_3}{k_6-k_3}\cdot\frac{\alpha_3 k_4}{k_4-k_3} \quad (3\to 4\ \overrightarrow{\alpha_3}\ 6)\\
&+ \frac{\alpha_1 k_3}{k_6-k_3}\cdot\frac{\alpha_2 k_4}{k_4-k_3}\cdot\frac{k_5}{k_5-k_3} \quad (3\to 4\ \overrightarrow{\alpha_2}\ 5\to 6)
\end{aligned}
$$

$$S_{6,4} = \frac{\alpha_3 k_4}{k_6 - k_4} \quad (4 \overrightarrow{\alpha_3} 6)$$
$$+ \frac{\alpha_2 k_4}{k_6 - k_4} \cdot \frac{k_5}{k_5 - k_4} \quad (4 \overrightarrow{\alpha_2} 5 \rightarrow 6).$$

References

Bateman, H., 1910, Solution of a system of differential equations occurring in the theory of radioactive transformations, *Proc. Cambridge Philos. Sco.*, **15**, 423–427.

Bowyer, T.W., Schlosser, C., Abel, K.H., Auer, M., Hayers, J.C., Heimbigner, T.R., McIntyre, J.I., Panisko, M.C., Reeder, P.L., Satorius, H., Schulze, J., Weiss, W., 2002, Detection and analysis of xenon isotopes for the comprehensive nuclear-test-ban treaty international monitoring system, *J. Environ. Radioac.*, **59**(2), 139–151.

Carrigan, C.R., Heinle, R.A., Hudson, G.B., Nitao, J.J., Zucca, J.J., 1996, Trace gas emissions on geological faults as indicators of underground nuclear testing, *Nature*, **382**(6591), 528–531, doi:10.1038/382528a0.

Carrigan, C.R., Sun, Y., 2012, Detection of noble gas radionuclides from an underground nuclear explosion during a CTBT on-site inspection, *Pure Appl. Geophys.*, 10.1007/s00024-012-0563-8.

Cetnar, J., 2006, General solution of Bateman equations for nuclear transmutations, *Ann. Nucl. Energy*, **33**, 640–645.

Clement, T.P., Sun, Y., Hooker, B.S., Petersen, J.N., 1998. Modeling multi-species reactive transport in groundwater aquifers. *Ground Water Monit. Remediat.*, **18**(2), 79–92.

England, T.R., Rider, B.F., 1994, ENDF-349 Evaluation and compilation of fission product yields 1993, Los Alamos National Laboratory, LA-UR-94-3106.

ENSDF, 2009, Evaluated Nuclear Structure Data File (ENSDF), National Nuclear Data Center at Brookhaven National Laboratory.

Hao, Y., Sun, Y., Nitao, J.J., 2012, Overview of NUFT – a versatile numerical model for simulating flow and reactive transport in porous media, Edited by Zhang et al. in *Ground water reactive transport model*, Bentham Science Publishers.

Lu, X., Sun, Y., Petersen, J.N., 2003, Analytical solutions of TCE transport with convergent reactions, *Transport Porous Med.*, **51**(3), 211–225.

Kalinowski, M.B., Pistner, C., 2006, Isotopic signature of atmospheric xenon released from light water reactors, *J. Environ. Radio.*, **88**(3), 215–235.

Kalinowski, M.B., Axelsson, A., Bean, M., Blanchard, X., Bowyer, T.W., Brachet, G., Hebel, S., McIntyre, J.I., Peters, J., Pistner, C., Raith, M., Ringbom, A., Saey, P., Schlosser, C., Stocki, T.J., Taffary, T., Ungar, R.K., 2010, Discrimination of nuclear explosions against civilian sources based on atmospheric xenon isotopic activity ratios, *Pure Appl. Geophys.*, **167**(4-5), 517–539.

Kalinowski, M.B., 2011, Characterisation of prompt and delayed atmospheric radioactivity releases from underground nuclear tests at Nevada as a function of release time, *J. Environ. Radio.*, **102**(9), 824–836.

Lowrey, J.D., Biegalski, S.R., Deinert, M.R., 2012, UTEX modeling of radioxenon isotopic fractionation resulting from a subsurface transport, *J. Radioanal. Nucl. Chem.*, doi:10.10007/s10967-012-2026-1.

Lowrey, J.D., Biegalski, S.R., Osborne, A.G., Deinert, M.R., 2013, Subsurface mass transport affects the radioxenon signatures that are used to identify clandestine nuclear tests, *Geophys. Res. Lett.*, **40**(1), 111–115, doi: 10.1029/2012GL053885.

MathWorks, 2000, *MATLAB high-performance numeric computation and visualization software*, Web site: www.mathwroks.com, Natick, MA, USA.

Moler, C., van Loan, C., 1978, Nineteen dubious ways to compute the exponential of a matrix, twenty-five years later, *SIAM Review*, **20**(3), 801–836.

Moral, L., Pacheco, A.F., 2003, Algebraic approach to the radioactive decay equation, *Am. J. Phys.*, **71**(7), 684–686.

Nitao, J.J., 1998. User's manual for the USNT module of the NUFT code, version 2 (NP-phase, NC-component, thermal), Lawrence Livermore National Laboratory, UCRL-MA-130653.

Pigford, T.H., Chambre, P.L., Albert, M., Foglia, M., Harada, M., Iwamoto, F., Kanki, T., Leung, D., Masuda, S., Muraoka, S., Ting, D., 1980, Migration of radionuclides through sorbing media: analytical solutions II, ONWI 360(1), LBL-11616, UCB-NE-4003.

Pressyanov, D.S., 2002, Short solution of the radioactive decay chain equations, *Am. J. Phys.*, **70**(4), 444–445.

Radhakrishnan, K., Hindmarsh, A.C., 1993, *Description and use of LSODE, the Livermore solver for ordinary differential equations*, Lawrence Livermore National Laboratory, report UCRL-ID-113855.

Saey, P.R.J., Bowyer, T.W., Ringbom, A., 2010, Isotopic noble gas signatures released from medical isotope production facilities Simulations and measurements, *Appl. Radiat. Isotopes*, **68**(9), 1846–1854.

Slodička, M., Balážová, A., 2008, Singular value decomposition method for multi-species first-order reactive transport with identical decay rates, *Transport Porous Med.*, **73**(2), 161-172.

Srinivasan, V., Clement, T.P., 2008, Analytical solutions for sequentially coupled one-dimensional reactive transport problems-Part I: Mathematical derivations, *Adv. Water Resour.*, **31**(2), 203–218.

Sun, Y., Petersen, J.N., Clement, T.P., Hooker, B.S., 1998, Effect of reaction kinetics on predicted concentration profiles during subsurface bioremediation, *J. Contam. Hydrol.*, **31**(3-4), 359–372.

Sun, Y., Clement, T.P., 1999, A decomposition method for solving coupled multi-species reactive transport problem, *Transport Porous Med.*, **37**(3), 327–346.

Sun, Y., Petersen, J.N., Clement, T.P., 1999a, Analytical solutions for multiple species reactive transport in multiple dimensions, *J. Contam. Hydrol.*, **35**(4), 429–440.

Sun, Y., Petersen, J.N., Clement, T.P., Skeen, R.S., 1999b, Development of analytical solutions for multi-species transport with serial and parallel reactions, *Water Resour. Res.*, **35**(1), 185–190.

Sun, Y., Buscheck, T.A., 2003, Analytical solutions for reactive transport of N-member radionuclide chains in a single fracture *J. Contam. Hydrol.*, **62-63**, 695–712.

Sun, Y., Lu, X., Petersen, J.N., Buscheck, T.A., 2004, An analytical solution of tetrachloroethylene transport and biodegradation, *Transport Porous Med.*, **55**(3), 301–308.

Sun, Y., Buscheck, T.A., Hao, Y., 2008, Modeling reactive transport using exact solutions for first-order reaction networks, *Transport Porous Med.*, **71**(2), 217–231.

Sun, Y., Buscheck, T.A., Lee, K.H., Hao, Y., James, S.C., 2010, Modeling thermal-hydrologic processes for a heated fractured rock system: impact of a capillary-pressure maximum, *Transport Porous Med.*, **83**(3), 501–523.

Sun, Y., Buscheck, T.A., Hao, Y., 2012, An analytical method for modeling first-order decay networks, *Comput. Geosci.*, **39**, 86–97, doi:10.1016/j.cageo.2011.06.015.

Sun, Y., Carrigan, C.R., 2012, Modeling noble gas transport and detection for the Comprehensive Nuclear-Test-Ban Treaty, *Pure Appl. Geophys.*, doi:10.1007/s00024-012-0514-4.

Thomas, G.F., Barber, D.H., 1994, Stiffness of radioactive decay chains, *Ann. Nucl. Energy*, **21**(5), 309–320.

van Genuchten, M.Th., 1985, Convective-dispersive transport of solutes involved in sequential first-order decay reactions, *Comput. Geosci.*, **11**(2), 129–147.

Xu, T., Sonnenthal, E., Spycher, N., Pruess, K., 2006, TOUGHREACT $\sim$ A simulation program for non-isothermal multiphase reactive geochemical transport in variably saturated geologic media: Applications to geothermal injectivity and CO_2 geological sequestration, *Comput. Geosci.*, **32**(2), 145–165.

Yuan, D., Kernan, W., 2007, Explicit solution for exit-only radioactive decay chains, *J. Appl. Phys.*, **101**(9), 094907.

This preprint was prepared with Yunwei Sun's LaTeX macros v4. File ratio4 formatted December 18, 2013.